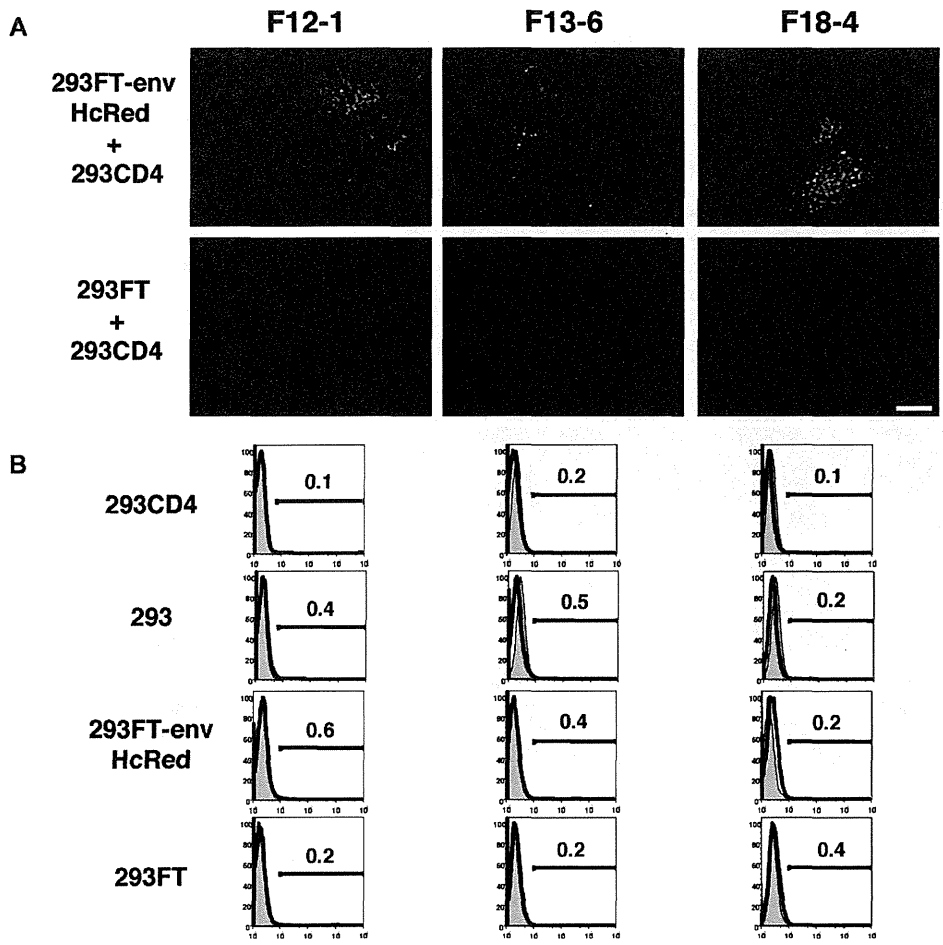

Fig. 3. Expression of epitopes recognized by mAbs. In the screening of mAbs (200 clones), mAbs from 23 clones with various isotypes are non-responding to either 293CD4 or 293FT-env (data not shown). (A) Three mAbs, F12-1, F13-6, and F18-4, showed the positive signals when cells are membrane fused compared with the negative control (293FT + 293CD4). Bars = 100 μm. (B) The mAbs were also examined on the individual cells by flow cytometric analysis. These results are representative of three independent experiments.

flow cytometry. Supernatants negative for both transfectants were chosen for further screening in co-culture of the transfectants. Positive hybridomas were re-cloned for confirmation of their binding specificities. Designated F12-1, F13-6 and F18-4 clones were chosen as three mAbs that recognize the epitopes apparently during the membrane fusion.

mAbs that recognized the antigenic epitopes of CD4 were screened by ELISA using soluble CD4 (R&D Systems, Minneapolis, MN). mAbs designated B224, R260, R210, R19, R35, B40, B211, R240 and R275 were characterized and found to recognize the extracellular region of human CD4 in the 293CD4 transfectants.

Commercially available fluorochrome Abs were: allophycocyanin- (eBioscience, San Diego, CA) and biotin-conjugated (Biolegend, San Diego, CA) OKT4, phycoerythrin (PE)-conjugated RPA-T4 (Biolegend), and fluorescein isothiocyanate (FITC)-conjugated CD3 (Beckman Coulter, Brea, CA). The anti-CD4 mAbs used were: RPA-T4 (Biolegend), S3.5 (Caltag Laboratories, Burlingame, CA), Leu-3a/SK3 (Biolegend), Q4120 (Sigma Aldrich), OKT4 (Biolegend), Leu-3a (BD Bioscience), and Leu-3 (eBioscience).

Immunocytostaining

Single transfectants without spGFP constructs included 293FT-env and 293CD4 which were used for vFC staining. Co-cultured cells were fixed with 0.2% formaldehyde-PBS for 2 h at 4 °C. mAbs (5 μg/ml) were added for 1 h at RT and detected with goat anti-mouse IgG conjugated to AlexaFluor® 488 under the conventional staining procedure.

Flow cytometric analysis

mAbs conjugated to biotin were used for staining the cell surface epitope by cross-inhibition with mAbs against known CD4 epitopes. The signal was detected with Streptavidin-PerCP Cy5.5 (BD Bioscience) or Streptavidin-PE Cy7 (eBioscience). Cells were analyzed using FACSCalibur (Becton Dickinson) or JSAN cell sorters (Bay Bioscience, Kobe, Japan) with FlowJo software (Tree Star, OR).

Virus neutralization assay

Recombinant luciferase-reporter virus stock pseudotyped with HIV-1 envelope was generated by co-transfection of 293T cells with pHIV-1 NL-Luc (Masuda et al., 1995) and pCXN2 vector expressing envelope from JR-FL (Maeda et al., 2000). The neutralization of pseudovirus infection by the mAb was measured using MAGI/CCR5 cells as previously described (Maeda et al., 2000). The infectious HIV-1 stocks of NL4-3 (Adachi et al., 1986),

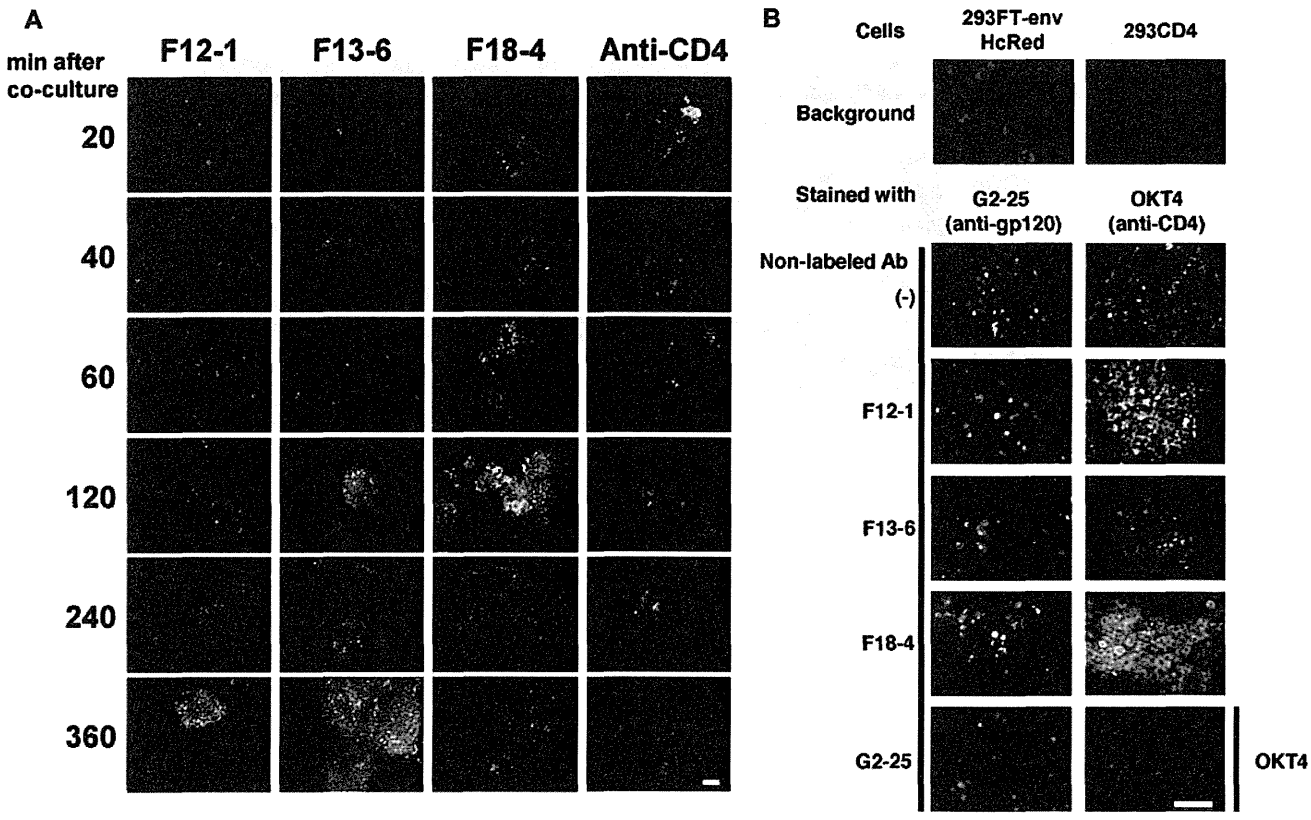

Fig. 4. Appearance of vFC epitopes and their association with membrane fusion and virus infection. (A) Kinetics of the appearance of vFC during co-culture of 293CD4 and 293FT-env cells. The signal was visualized using the mAbs plus AlexaFluor 488-anti-mIg Abs after fixation. All images are the same size and each experiment was repeated three times with identical results. Bars = 100 μm. (B) Effect of anti-vFC mAb on epitopes within Env and CD4. 293FT-env HcRed cells were preincubated with the anti-vFC mAbs for 1 h at RT, lightly washed with PBS, and stained with biotinylated G2-25 without fixation. 293CD4 cells were processed similarly and stained with FITC-labeled OKT4. The specific signals were confirmed using non-labeled mAbs, G2-25 and OKT4. Bars = 100 μm. These results are representative of three independent experiments.

JR-FL (Koyanagi et al., 1987), 89.6 (Collman et al., 1992) and Indie-C1 (Mochizuki et al., 1999) were prepared using 293T cells by transfection. The HIV-1 stock of BaL (Gartner et al., 1986) was prepared from the culture supernatant of PM1/CCR5 cells (Yusa et al., 2005) infected with BaL. For the neutralization assay, we used a TZM-bl cell line expressing CD4 and CXCR4/CCR5 and carrying the luciferase and β-galactosidase reporter genes under the control of HIV-1 LTR (Platt et al., 1998; Wei et al., 2002). Briefly, TZM-bl cells (1×10^4) were infected with aforementioned infectious viruses in the presence of the mAb (0.5, 5, and 50 μg/ml) and the luciferase activities were measured 48 h after infection. Inhibitory concentration (IC_{50}) value was calculated as the concentration of mAb giving 50% of relative luminescence units (RLUs) compared with those of virus control after subtraction of background RLUs.

$NaIO_4$-treatment and cross-inhibition using known mAbs

After fixation with 4% paraformaldehyde-PBS for 15 min at RT, 293CD4 cells were treated with 20 mM sodium periodate in 0.1 M sodium acetate buffer pH 5.5 for 15 min at RT. The deglycosylated 293CD4 cells were stained with R275 and analyzed by FACS. Cross-inhibition was performed to determine the epitope for R275. After a 1 h incubation with unlabeled mAb (25 μg/ml) at 4 °C, 293CD4 cells were stained with biotinylated R275 followed by Streptavidin-PE Cy7.

Results

Establishment of mAbs against the epitopes during vFC formation using GANP^{Tg} mice

The spGFP system (Fig. 1A) (Wang et al. 2009) was used to prepare vFC. 293FT cells were transfected to express HIV-1 Env + HcRed plus a fragment of the GFP protein (GFP_{11}) linked to the membrane-targeting pleckstrin homology (PH) domain of human phospholipase C δ (293FT-env^{GFP11}). Host 293 cells expressing CXCR4 were transfected with human *cd4* cDNA and a large fragment of the *gfp* gene (regions 1–10) linked to the PH region (293CD4$^{GFP1-10}$). When both cells fuse to form vFC-like structures, the fused membrane emits the green fluorescence signal together with nucleus-targeted HcRed (Fig. 1B). Images were recorded 20–40 min after the start of co-culture. The membrane-fused cells were fixed with 0.2% formaldehyde in PBS at 15 min and used as the immunogen. Hybridoma cells secreting anti-vFC mAbs were established using conventional cell fusion of P3U1 cells with splenocytes from GANP^{Tg} mice immunized with the vFC.

We obtained nine mAbs against CD4 by screening with human CD4 expressed on the surface of transfectants (Fig. 2A). Eight anti-CD4 mAb clones recognized peptide sequences within extracellular CD4 other than the D1 and D2 sequences known to interact with the Env protein and MHC class II (Fig. 2B and C).

Fluorescence microscopy showed that mAb-producing clones, designated F12-1, F13-6, and F18-4, selectively bound to the vFC

created between 293FT-env- and 293CD4-transfectants (Fig. 3A). None of these mAbs reacted with 293CD4 or 293FT-env cells (Fig. 3B), indicating that they did not recognize the Env protein or the CD4 protein expressed alone on the cell membrane. The mAbs recognized the membrane vFC formed between 293FT-env and 293CD4 cells, but did not recognize 293CD4 (negative control) cells.

Altered appearance of vFC epitopes recognized by the mAbs

The appearance of antigenic epitopes was examined under fluorescence microscopy after co-culturing 293FT-env and 293CD4 cells (Fig. 4A). F12-1 and F13-6 recognized epitopes appearing at later time points on cells expressing env-HcRed signals. The vFC epitopes appeared at different time points during fusion: the F18-4 epitope appeared relatively early (120 min at the latest); the F13-6 epitope appeared when Env interacted with CD4, creating and stabilizing the vFC. Finally, the F12-1 epitope appeared after 360 min.

CD4 epitope expression may also vary during the process of membrane fusion. We next studied whether the anti-vFC mAbs caused alterations in the epitope appearance within CD4 or Env that are expressed on the cell surface prior to their interaction. Pre-incubation of 293FT-env cells with non-labeled anti-vFC mAbs did not cause any change in the binding of G2-25 (Fig. 4B). However, pretreatment of 293CD4 cells with F12-1 or F18-4 resulted in enhanced OKT4 binding, suggesting that some of the anti-vFC mAbs have partial affinity for CD4, and the binding may cause the exposure of OKT4-antigenic epitope on the global surface of CD4 molecule.

Inhibition of membrane fusion by anti-vFC mAbs

We examined the effects of the mAbs on the formation of vFC and membrane fusion. 293FT-env^{GFP11} and 293CD4$^{GFP1-10}$ were co-cultured in the presence of excess F12-1, F13-6, or F18-4. The GFP fusion signal on co-cultured cells was then examined (Fig. 5). G2-25, directed against the V3-epitope of gp120, markedly suppressed the GFP signal at 6 h (Fig. 5A), and this tendency continued up until 12 h (Fig. 5B). MAbs F12-1, F13-6, and F18-4 modestly inhibited membrane fusion (Fig. 5A and B). However, the anti-CD4 mAb R275 inhibited membrane fusion to the same extent as anti-gp120 mAb G2-25. In addition, R275 showed marked inhibition of membrane fusion in the luciferase assay compared with mAbs against CD4, including the ones with anti-D3 region of CD4 (Figs. 2C and 5C).

Analysis of the epitope recognized by R275 anti-CD4 mAb

R275 reacted with extracellular CD4 on cells and with recombinant soluble CD4 (R&D systems), but not with recombinant CD4 protein produced in *Escherichia coli* (Fig. 2). This suggests that R275 recognizes glycosylation or conformational epitopes. To examine this, CD4-transfected cells were treated with $NaIO_4$. The results showed that $NaIO_4$ had little effect upon R275 binding; similar results were obtained for R240 (Fig. 6A). No inhibition by mAbs recognizing the D1 region of CD4 was detected (RPA-T4, S3.5, SK3/Leu3a, and Q4120) (Healey et al. 1990); however, OKT4, which recognizes the D3 region, showed clear inhibition of R275 binding to CD4 on the cell surface (Fig. 6B). Therefore, we further analyzed the epitope expressed by human OKT4-non-reactive CD4$^+$ T cells recognized by R275. A single aa mutation (at aa 265) abrogated the binding of OKT4 mAb (Lederman et al. 1991). R275 staining of CD4$^+$ T cells isolated from OKT4 epitope-positive and -negative individuals was then examined. The results showed that R275 only weakly recognized OKT4 non-reactive CD4$^+$ T cells (Fig. 6C),

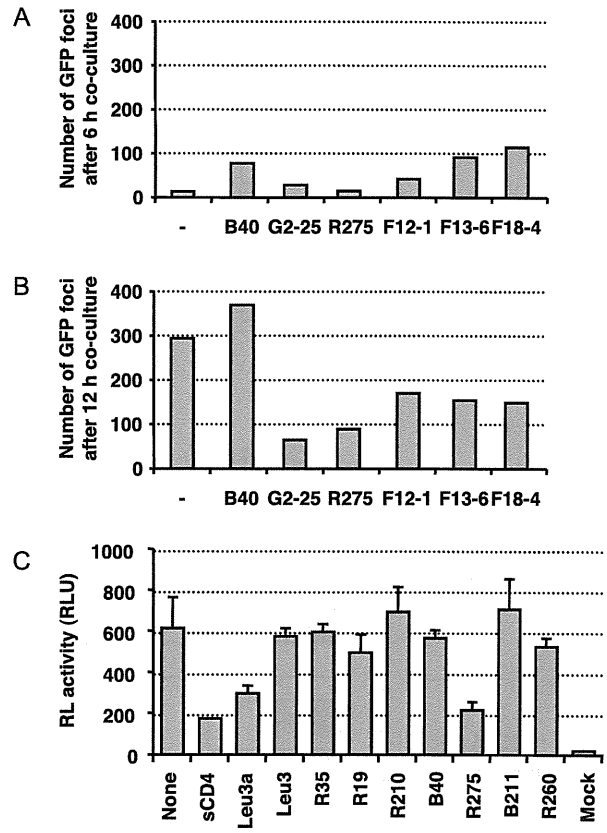

Fig. 5. Effect of the mAbs on membrane fusion. The effects on membrane fusion were measured using the spGFP system. (A) The green fluorescent foci with HcRed signals were counted in the total culture (1×10^5 cells) from each group after 6 h and (B) 12 h. (C) Membrane fusion was measured using the split fusion assay. The positive controls were soluble CD4 (10 μg/ml) and Leu3a mAb. These results are representative of three independent experiments.

indicating that the R275 epitope may not be identical to, but closely associated with, the OKT4 epitope on the D3 region.

Neutralizing activity in the HIV-1 infection assay

The neutralizing activity of the mAbs was measured by using a pseudovirus assay incorporating MAGI-CCR5 cells (Maeda et al. 2000, 2008) (Fig. 7A). None of the anti-vFC mAbs (F12-1, F13-6, or F18-4) inhibited viral infection when compared with the anti-Env mAb, G2-25. None of the mAbs directed against the extracellular domain of CD4 (other than the D1 and D2 regions) showed virus neutralization activity, apart from R275, which recognized the native form of the extracellular region of CD4 expressed on the surface of CD4-transfectants (Fig. 7B).

Only Leu3a (which binds to the D1 region) and R275 showed marked inhibition of viral infection comparable to that of soluble CD4. No other anti-D3 mAb showed such inhibition; indeed, R210 and B211 occasionally enhanced infectivity. Similarly, F12-1, F13-6, and F18-4 appeared to enhance viral infection. The molecular mechanisms underlying these adverse effects are unclear; therefore, careful investigation of these effects is needed if the prevention of viral infection is to be a specific target for AIDS vaccines.

The IC_{50} for viral infection of TZM-bl cells showed that R275 inhibited the infectivity of NL43 (clade B), 89.6 (clade B), and Indie-C1 (clade C) viruses (each displaying different CXCR4/CCR5 usage) at doses of around 10 μg/ml; however, it was less effective against BaL (clade B), which is resistant to soluble CD4-mediated

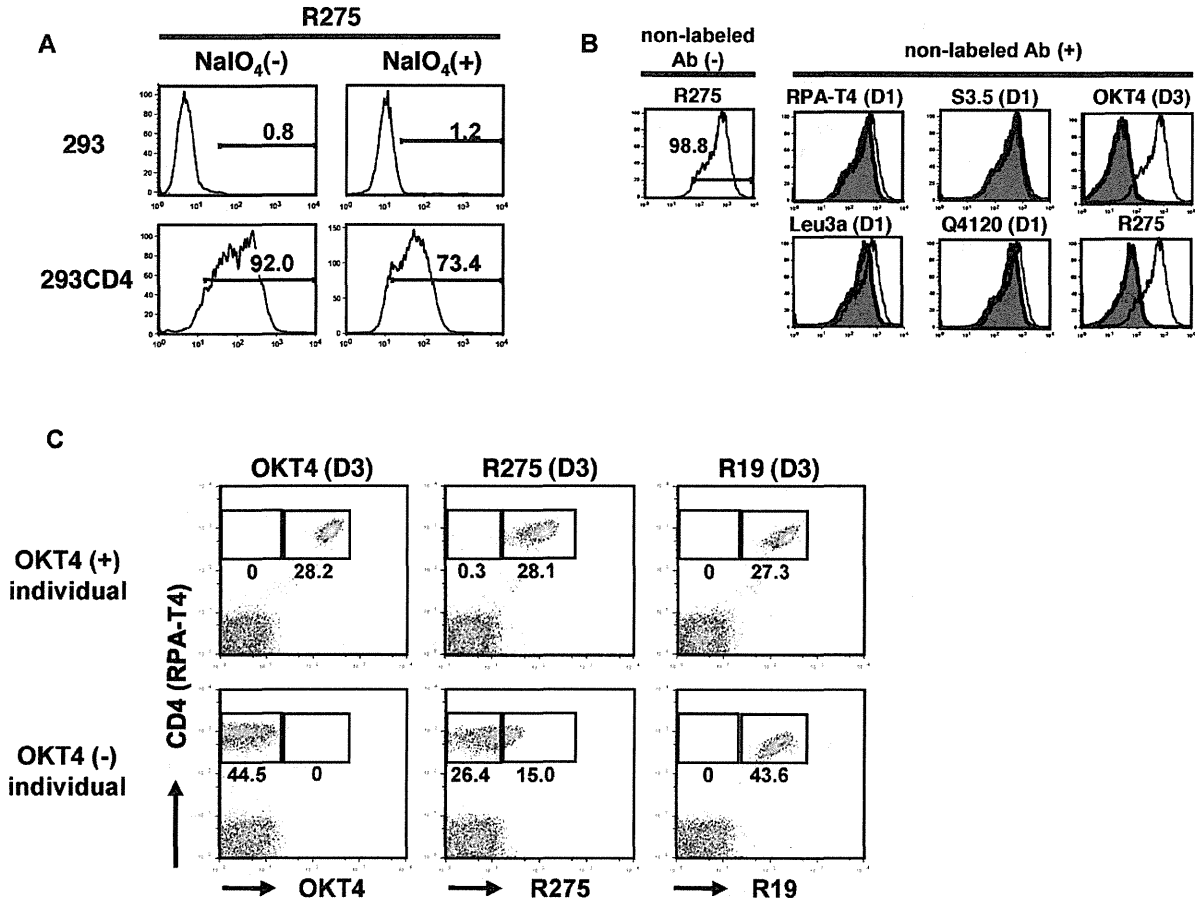

Fig. 6. Analysis of the R275 epitope. CD4-transfectants were treated with $NaIO_4$ and stained with R240 or R275. (A) $NaIO_4$, which destroys the antigenicity of sugar epitopes, did not result in marked changes in R275 binding. (B) Cross-inhibition using known mAbs showed that OKT4 (directed against the D3 region) inhibited the binding of R275, but not binding of the other mAbs. (C) OKT4-negative individuals showed decreased expression of the R275 epitope on T cells. These results are representative of three independent experiments.

prevention (Fig. 7C). These results highlight the relative breadth of anti-viral infection activity.

Discussion

R275 showed marked neutralization activity (65–80% inhibition) in the *in vitro* pseudovirus infection assay at a dose of 0.5 μg, but this effect did not reach 100%, even when the dose was increased to 50 μg (Fig. 7B). This suggests that viral infection proceeds through a complex formed via structural changes at the different interaction sites. R275 epitopes (other than the D1 and D2 regions) are globally expressed on the surface of the CD4 molecule, and may participate in the crucial process of vFC formation during membrane fusion and affect viral infection.

A previous report by Healey et al. (1990) showed that mAb Q425, which recognizes a 249–252 aa region within the D3 region of CD4, showed broadly neutralizing activity and the supposed inhibition of membrane fusion. The D3 region of CD4 is not involved in the initial interaction with either gp120 or MHC class II, but may be involved in the subsequent process of membrane fusion. The data presented in this study, along with those for Q425, provide valuable information regarding the very early stages of membrane fusion after the initial interaction between Env and CD4. A crystallographic model reported by Wu and colleagues shows that the R275 epitope is also confined to the D3 region of CD4 based on the information of OKT4-recognition region spanning 265 aa (Wu et al. 1997).

Vaccination with high-affinity Abs against HIV-1 will provide efficient protection against virus infection and augment immune responses. Several challenging studies show that mAbs specific for vFC epitopes can be generated, and that they are able to prevent virus infection. The epitopes recognized by such mAbs presumably reside within the region(s) critical for the membrane fusion and, therefore, are expected to be less mutated during treatment. In this study, we attempted to examine whether such unique antigenic epitopes are in fact generated within the vFC complex during membrane fusion. By visualizing the appearance of the vFC, we obtained three mAbs that selectively recognize epitopes on the vFC-like structure, which appear at different time points during membrane fusion and may affect the exposure of CD4 epitope (Fig. 4). However, all three mAbs recognized epitopes that appear during the later stages of membrane fusion and, therefore, they are expected to be less effective at preventing this process, and to have little effect on viral infection. In contrast, a mAb recognizing the D3 region of CD4 appeared to be effective at inhibiting both membrane fusion and viral infection. The D3 region may interact with the Env protein during membrane fusion, resulting in dynamic alterations in the trimer complex. Alternatively, the mAb binding to the region in vFC other than the CD4 D1 region may cause changes of the trimer complex involved in virus infection as proposed in a model with anti-env 17b mAb (Pancera et al., 2010). Interestingly, the interaction between the F12-1 or F18-4 epitopes and the D3 OKT4 epitope of CD4 might generate potential targets for the prevention of

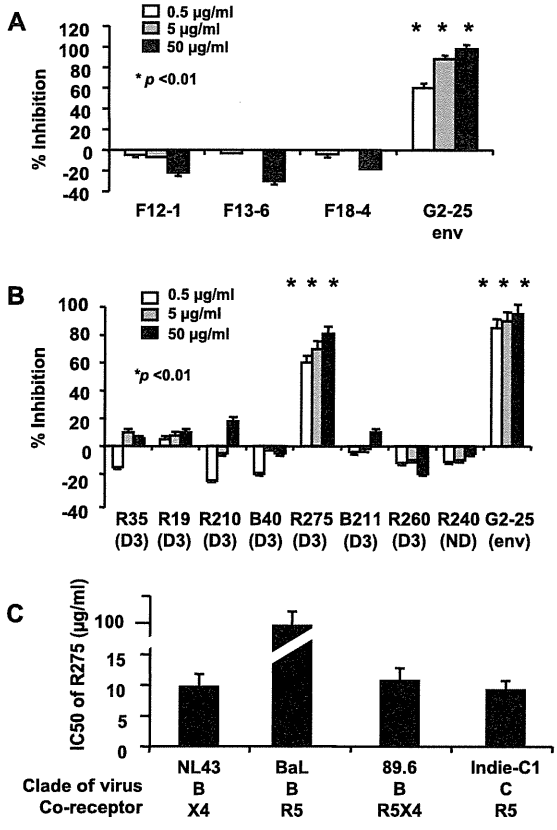

Fig. 7. Effect of the mAbs on viral infectivity. (A and B) Inhibition of virus infection by the purified mAbs was measured using a pseudovirus infection assay. The effect was compared with that of a control mAb directed against the V3-epitope of NL43 Env (G2-25). The p value was compared for the neutralizing activity between isotype control mouse IgG and anti-vFC mAbs, anti-CD4 mAbs or the G2-25 mAb using Student's t-test. $^*p < 0.01$. (C) Virus neutralization of R275 was measured using various clades of HIV-1. IC50 value was determined. These results are representative of three independent experiments.

membrane fusion and viral neutralization. The mAbs described in the present study may distinguish and define the epitopes appearing during the process of membrane fusion and provide an opportunity for preventing viral infection. Taken together, the results of this study will contribute to the future design of effective HIV vaccines.

Acknowledgments

The following reagents were obtained through the NIH AIDS Research and Reference Reagent Program, Division of AIDS, NIAID, NIH: TZM-bl from Dr. John C. Kappes, Dr. Xiaoyun Wu and Tranzyme Inc., pNL4-3 from Dr. Malcolm Martin, p89.6 from Ronald G. Collman, HIV-1_{Ba-L} from Dr. Suzanne Gartner, Dr. Mikulas Popovic and Dr. Robert Gallo. We also thank Dr. Irvin S. Chen, Dr. Yoshio Koyanagi, and Dr. Masashi Tatsumi for kindly providing HIV NL-Luc plasmid, JR-FL plasmid, Indie-C1 plasmid, respectively, and Ms. Mika Ito for assistance.

References

Adachi, A., Gendelman, H.E., Konig, S., Folks, T., Willey, R., Rabson, A., Martin, M.A., 1986. Production of acquired immunodeficiency syndrome-associated retrovirus in human and nonhuman cells transfected with an infectious molecular clone. J. Virol. 59, 284–291.

Arthos, J., Deen, K.C., Chaikin, M.A., Fornwald, J.A., Sathe, G., Sattentau, Q.J., Clapham, P.R., Weiss, R.A., McDougal, J.S., Pietropaolo, C., Axel, R., Truneh, A., Maddon, P.J., Sweet, R.W., 1989. Identification of the residues in human CD4 critical for the binding of HIV. Cell 57, 469–481.

Berger, E.A., Murphy, P.M., Farber, J.M., 1999. Chemokine receptors as HIV-1 coreceptors: roles in viral entry, tropism, and disease. Annu. Rev. Immunol. 17, 657–700.

Burton, D.R., Pyati, J., Koduri, R., Sharp, S.J., Thornton, G.B., Parren, P.W., Sawyer, L.S., Hendry, R.M., Dunlop, N., Nara, P.L., et al., 1994. Efficient neutralization of primary isolates of HIV-1 by a recombinant human monoclonal antibody. Science 266, 1024–1027.

Camerini, D., Seed, B., 1990. A CD4 domain important for HIV-mediated syncytium formation lies outside the virus binding site. Cell 60, 747–754.

Chan, D.C., Kim, P.S., 1998. HIV entry and its inhibition. Cell 93, 681–684.

Choe, H., Li, W., Wright, P.L., Vasilieva, N., Venturi, M., Huang, C.C., Grundner, C., Dorfman, T., Zwick, M.B., Wang, L., Rosenberg, E.S., Kwong, P.D., Burton, D.R., Robinson, J.E., Sodroski, J.G., Farzan, M., 2003. Tyrosine sulfation of human antibodies contributes to recognition of the CCR5 binding region of HIV-1 gp120. Cell 114, 161–170.

Collman, R., Balliet, J.W., Gregory, S.A., Friedman, H., Kolson, D.L., Nathanson, N., Srinivasan, A., 1992. An infectious molecular clone of an unusual macrophage-tropic and highly cytopathic strain of human immunodeficiency virus type 1. J. Virol. 66, 7517–7521.

Decker, J.M., Bibollet-Ruche, F., Wei, X., Wang, S., Levy, D.N., Wang, W., Delaporte, E., Peeters, M., Derdeyn, C.A., Allen, S., Hunter, E., Saag, M.S., Hoxie, J.A., Hahn, B.H., Kwong, P.D., Robinson, J.E., Shaw, G.M., 2005. Antigenic conservation and immunogenicity of the HIV coreceptor binding site. J. Exp. Med. 201, 1407–1419.

Diskin, R., Marcovecchio, P.M., Bjorkman, P.J., 2010. Structure of a clade C HIV-1 gp120 bound to CD4 and CD4-induced antibody reveals anti-CD4 polyreactivity. Nat. Struct. Mol. Biol. 17, 608–613.

Doms, R.W., Moore, J.P., 2000. HIV-1 membrane fusion: targets of opportunity. J. Cell Biol. 151, F9–F14.

Eckert, D.M., Kim, P.S., 2001. Mechanisms of viral membrane fusion and its inhibition. Annu. Rev. Biochem. 70, 777–810.

Eda, Y., Murakami, T., Ami, Y., Nakasone, T., Takizawa, M., Someya, K., Kaizu, M., Izumi, Y., Yoshino, N., Matsushita, S., Higuchi, H., Matsui, H., Shinohara, K., Takeuchi, H., Koyanagi, Y., Yamamoto, N., Honda, M., 2006a. Anti-V3 humanized antibody KD-247 effectively suppresses ex vivo generation of human immunodeficiency virus type 1 and affords sterile protection of monkeys against a heterologous simian/human immunodeficiency virus infection. J. Virol. 80, 5563–5570.

Eda, Y., Takizawa, M., Murakami, T., Maeda, H., Kimachi, K., Yonemura, H., Koyanagi, S., Shiosaki, K., Higuchi, H., Makizumi, K., Nakashima, T., Osatomi, K., Tokiyoshi, S., Matsushita, S., Yamamoto, N., Honda, M., 2006b. Sequential immunization with V3 peptides from primary human immunodeficiency virus type 1 produces cross-neutralizing antibodies against primary isolates with a matching narrow-neutralization sequence motif. J. Virol. 80, 5552–5562.

Finnegan, C.M., Berg, W., Lewis, G.K., DeVico, A.L., 2001. Antigenic properties of the human immunodeficiency virus envelope during cell–cell fusion. J. Virol. 75, 11096–11105.

Gartner, S., Markovits, P., Markovitz, D.M., Kaplan, M.H., Gallo, R.C., Popovic, M., 1986. The role of mononuclear phagocytes in HTLV-III/LAV infection. Science 233, 215–219.

Haim, H., Steiner, I., Panet, A., 2007. Time frames for neutralization during the human immunodeficiency virus type 1 entry phase, as monitored in synchronously infected cell cultures. J. Virol. 81, 3525–3534.

Healey, D., Dianda, L., Moore, J.P., McDougal, J.S., Moore, M.J., Estess, P., Buck, D., Kwong, P.D., Beverley, P.C., Sattentau, Q.J., 1990. Novel anti-CD4 monoclonal antibodies separate human immunodeficiency virus infection and fusion of CD4+ cells from virus binding. J. Exp. Med. 172, 1233–1242.

Kondo, N., Miyauchi, K., Meng, F., Iwamoto, A., Matsuda, Z., 2010. Conformational changes of the HIV-1 envelope protein during membrane fusion are inhibited by the replacement of its membrane-spanning domain. J. Biol. Chem. 285, 14681–14688.

Koyanagi, Y., Miles, S., Mitsuyasu, R.T., Merrill, J.E., Vinters, H.V., Chen, I.S., 1987. Dual infection of the central nervous system by AIDS viruses with distinct cellular tropisms. Science 236, 819–822.

Labrijn, A.F., Poignard, P., Raja, A., Zwick, M.B., Delgado, K., Franti, M., Binley, J., Vivona, V., Grundner, C., Huang, C.C., Venturi, M., Petropoulos, C.J., Wrin, T., Dimitrov, D.S., Robinson, J., Kwong, P.D., Wyatt, R.T., Sodroski, J., Burton, D.R., 2003. Access of antibody molecules to the conserved coreceptor binding site on glycoprotein gp120 is sterically restricted on primary human immunodeficiency virus type 1. J. Virol. 77, 10557–10565.

Lederman, S., DeMartino, J.A., Daugherty, B.L., Foeldvari, I., Yellin, M.J., Cleary, A.M., Berkowitz, N., Lowy, I., Braunstein, N.S., Mark, G.E., et al., 1991. A single amino acid substitution in a common African allele of the CD4 molecule ablates binding of the monoclonal antibody OKT4. Mol. Immunol. 28, 1171–1181.

Maeda, K., Singh, S.K., Eda, K., Kitabatake, M., Pham, P., Goodman, M.F., Sakaguchi, N., 2010. GANP-mediated recruitment of activation-induced cytidine deaminase to cell nuclei and to immunoglobulin variable region DNA. J. Biol. Chem. 285, 23945–23953.

Maeda, Y., Foda, M., Matsushita, S., Harada, S., 2000. Involvement of both the V2 and V3 regions of the CCR5-tropic human immunodeficiency virus type 1 envelope in reduced sensitivity to macrophage inflammatory protein 1alpha. J. Virol. 74, 1787–1793.

Maeda, Y., Yusa, K., Harada, S., 2008. Altered sensitivity of an R5X4 HIV-1 strain 89.6 to coreceptor inhibitors by a single amino acid substitution in the V3 region of gp120. Antiviral. Res. 77, 128–135.

Masuda, T., Planelles, V., Krogstad, P., Chen, I.S., 1995. Genetic analysis of human immunodeficiency virus type 1 integrase and the U3 att site: unusual phenotype of mutants in the zinc finger-like domain. J. Virol. 69, 6687–6696.

Miyauchi, K., Komano, J., Yokomaku, Y., Sugiura, W., Yamamoto, N., Matsuda, Z., 2005. Role of the specific amino acid sequence of the membrane-spanning domain of human immunodeficiency virus type 1 in membrane fusion. J. Virol. 79, 4720–4729.

Mochizuki, N., Otsuka, N., Matsuo, K., Shiino, T., Kojima, A., Kurata, T., Sakai, K., Yamamoto, N., Isomura, S., Dhole, T.N., Takebe, Y., Matsuda, M., Tatsumi, M., 1999. An infectious DNA clone of HIV type 1 subtype C. AIDS Res. Hum. Retroviruses 15, 1321–1324.

Muster, T., Steindl, F., Purtscher, M., Trkola, A., Klima, A., Himmler, G., Ruker, F., Katinger, H., 1993. A conserved neutralizing epitope on gp41 of human immunodeficiency virus type 1. J. Virol. 67, 6642–6647.

Ono, M., Matsubara, J., Honda, K., Sakuma, T., Hashiguchi, T., Nose, H., Nakamori, S., Okusaka, T., Kosuge, T., Sata, N., Nagai, H., Ioka, T., Tanaka, S., Tsuchida, A., Aoki, T., Shimahara, M., Yasunami, Y., Itoi, T., Moriyasu, F., Negishi, A., Kuwabara, H., Shoji, A., Hirohashi, S., Yamada, T., 2009. Prolyl 4-hydroxylation of alpha-fibrinogen: a novel protein modification revealed by plasma proteomics. J. Biol. Chem. 284, 29041–29049.

Pancera, M., Majeed, S., Ban, Y.E., Chen, L., Huang, C.C., Kong, L., Kwon, Y.D., Stuckey, J., Zhou, T., Robinson, J.E., Schief, W.R., Sodroski, J., Wyatt, R., Kwong, P.D., 2010. Structure of HIV-1 gp120 with gp41-interactive region reveals layered envelope architecture and basis of conformational mobility. Proc. Natl. Acad. Sci. U.S.A. 107, 1166–1171.

Platt, E.J., Wehrly, K., Kuhmann, S.E., Chesebro, B., Kabat, D., 1998. Effects of CCR5 and CD4 cell surface concentrations on infections by macrophagetropic isolates of human immunodeficiency virus type 1. J. Virol. 72, 2855–2864.

Ryu, S.E., Kwong, P.D., Truneh, A., Porter, T.G., Arthos, J., Rosenberg, M., Dai, X.P., Xuong, N.H., Axel, R., Sweet, R.W., Hendrickson, W.A., 1990. Crystal structure of an HIV-binding recombinant fragment of human CD4. Nature 348, 419–426.

Sakaguchi, N., Kimura, T., Matsushita, S., Fujimura, S., Shibata, J., Araki, M., Sakamoto, T., Minoda, C., Kuwahara, K., 2005. Generation of high-affinity antibody against T cell-dependent antigen in the Ganp gene-transgenic mouse. J. Immunol. 174, 4485–4494.

Sakaguchi, N., Maeda, K., Kuwahara, K., 2011. Molecular mechanism of immunoglobulin V-region diversification regulated by transcription and RNA metabolism in antigen-driven B cells. Scand. J. Immunol. 73, 520–526.

Sakaguchi, N., Toda, T., Nakaya, T., Kitabatake, M., Maeda, K., Kuwahara, K., 2009. Generation of high affinity monoclonal antibodies for the prevention of HIV infection. Recent Pat. DNA Gene Seq. 3, 88–95.

Sattentau, Q.J., Moore, J.P., Vignaux, F., Traincard, F., Poignard, P., 1993. Conformational changes induced in the envelope glycoproteins of the human and simian immunodeficiency viruses by soluble receptor binding. J. Virol. 67, 7383–7393.

Sattentau, Q.J., Weiss, R.A., 1988. The CD4 antigen: physiological ligand and HIV receptor. Cell 52, 631–633.

Thali, M., Moore, J.P., Furman, C., Charles, M., Ho, D.D., Robinson, J., Sodroski, J., 1993. Characterization of conserved human immunodeficiency virus type 1 gp120 neutralization epitopes exposed upon gp120-CD4 binding. J. Virol. 67, 3978–3988.

Trkola, A., Pomales, A.B., Yuan, H., Korber, B., Maddon, P.J., Allaway, G.P., Katinger, H., Barbas 3rd, C.F., Burton, D.R., Ho, D.D., et al., 1995. Cross-clade neutralization of primary isolates of human immunodeficiency virus type 1 by human monoclonal antibodies and tetrameric CD4-IgG. J. Virol. 69, 6609–6617.

Wang, J., Kondo, N., Long, Y., Iwamoto, A., Matsuda, Z., 2009. Monitoring of HIV-1 envelope-mediated membrane fusion using modified split green fluorescent proteins. J. Virol. Methods 161, 216–222.

Wang, J.H., Yan, Y.W., Garrett, T.P., Liu, J.H., Rodgers, D.W., Garlick, R.L., Tarr, G.E., Husain, Y., Reinherz, E.L., Harrison, S.C., 1990. Atomic structure of a fragment of human CD4 containing two immunoglobulin-like domains. Nature 348, 411–418.

Wei, X., Decker, J.M., Liu, H., Zhang, Z., Arani, R.B., Kilby, J.M., Saag, M.S., Wu, X., Shaw, G.M., Kappes, J.C., 2002. Emergence of resistant human immunodeficiency virus type 1 in patients receiving fusion inhibitor (T-20) monotherapy. Antimicrob. Agents Chemother. 46, 1896–1905.

Wu, H., Kwong, P.D., Hendrickson, W.A., 1997. Dimeric association and segmental variability in the structure of human CD4. Nature 387, 527–530.

Wyatt, R., Moore, J., Accola, M., Desjardin, E., Robinson, J., Sodroski, J., 1995. Involvement of the V1/V2 variable loop structure in the exposure of human immunodeficiency virus type 1 gp120 epitopes induced by receptor binding. J. Virol. 69, 5723–5733.

Xiang, S.H., Doka, N., Choudhary, R.K., Sodroski, J., Robinson, J.E., 2002. Characterization of CD4-induced epitopes on the HIV type 1 gp120 envelope glycoprotein recognized by neutralizing human monoclonal antibodies. AIDS Res. Hum. Retroviruses 18, 1207–1217.

Yusa, K., Maeda, Y., Fujioka, A., Monde, K., Harada, S., 2005. Isolation of TAK-779-resistant HIV-1 from an R5 HIV-1 GP120 V3 loop library. J. Biol. Chem. 280, 30083–30090.

Zolla-Pazner, S., O'Leary, J., Burda, S., Gorny, M.K., Kim, M., Mascola, J., McCutchan, F., 1995. Serotyping of primary human immunodeficiency virus type 1 isolates from diverse geographic locations by flow cytometry. J. Virol. 69, 3807–3815.

Jpn J Ophthalmol
DOI 10.1007/s10384-012-0174-z

CLINICAL INVESTIGATION

Broad-range real-time PCR assay for detection of bacterial DNA in ocular samples from infectious endophthalmitis

Manabu Ogawa · Sunao Sugita · Norio Shimizu · Ken Watanabe · Ichiro Nakagawa · Manabu Mochizuki

Received: 18 January 2012 / Accepted: 5 July 2012

Abstract
Background To evaluate a broad-range real-time polymerase chain reaction (PCR) targeting the bacterial 16S rRNA gene for detection of bacterial DNA in infectious endophthalmitis.
Methods The bacterial 16S rRNA gene was measured by quantitative real-time PCR. For the assay, bacterial DNA was prepared from 12 Gram-positive and 4 Gram-negative strains. To determine the optimum method for DNA extraction, four extraction procedures were selected by using DNA extraction program cards with and without the use of lysozyme. To evaluate PCR sensitivity, PCR fragments were amplified from *Staphylococcus aureus* and *Escherichia coli* DNA.
Results DNA extraction using the Bacteria card® without enzymes resulted in detection of all the tested strains at concentrations $\geq 10^7$ copies/mL. Extraction with the Bacteria card® with lysozyme resulted in detection of all the tested strains at concentrations $\geq 10^6$ copies/mL, indicative of no significant difference between the two procedures. DNA extraction using the Virus card®, both with and without enzymes, resulted in reduced efficiency of detection of all strains compared with use of the Bacteria card®. The PCR could detect as few as 1–10 colony-forming units (CFU) in diluted vitreous samples per reaction, and all tested bacterial species known to cause endophthalmitis were detected.
Conclusions Bacterial 16S-specific PCR can comprehensively detect the main causative bacteria of clinically suspected endophthalmitis.

Keywords Endophthalmitis · Bacteria · Polymerase chain reaction

M. Ogawa · S. Sugita · M. Mochizuki
Department of Ophthalmology and Visual Science, Graduate School of Medical and Dental Sciences, Tokyo Medical and Dental University, Tokyo, Japan

S. Sugita (✉)
Laboratory for Retinal Regeneration, RIKEN Center for Developmental Biology, 2-2-3 Minatojima-minamimachi, Chuo-ku, Kobe 650-0047, Japan
e-mail: sunaoph@cdb.riken.jp

N. Shimizu · K. Watanabe
Division of Medical Science, Department of Virology, Graduate School of Medical and Dental Sciences, Tokyo Medical and Dental University, Tokyo, Japan

I. Nakagawa
Department of Section of Bacterial Pathogenesis, Graduate School of Medicine and Dental Sciences, Tokyo Medical and Dental University, Tokyo, Japan

Introduction

Infectious bacterial endophthalmitis can result both from exogenous infections, for example exposure to infectious agents, trauma, and intraocular surgery, and endogenous infections, for example systemic infectious disorders. It is often difficult to differentiate between inflammation in ocular inflammatory disorders, for example infectious endophthalmitis caused by non-infectious and infectious agents. The standard for diagnosis of invasive bacterial infections used to be microscopic examination and conventional bacterial culture. Although microscopic examination is rapid, the smear test requires a relatively large concentration of bacteria, $\geq 10^4$ colony-forming units (CFU)/mL, to give a positive result [1]. Moreover, identification based solely on morphology is often not possible. Bacterial cultures are often used for differential diagnosis,

Published online: 31 August 2012

but there are several disadvantages, for example cultivation time (24–72 h) and low sensitivity. Inappropriate treatment because of misdiagnosis of infectious endophthalmitis can result in severe tissue damage and vision loss. Because of the difficulty of making proper diagnoses on the basis of the small amounts of ocular samples available, there is a need to consider the collection and preservation of clinical samples, including bacterial DNA, available for diagnostic use. Moreover, some cases involve rapid progression of the ocular infectious disease; therefore, accurate, rapid and comprehensive diagnosis is of great importance.

Polymerase chain reaction (PCR) is used for detection of bacteria in suspected intraocular infections [2–4]. Bacterial PCR is a diagnostic tool that can be used for detection in intraocular specimens, and can be used as an alternative tool for subsequent examination of specimens found to be bacteriologically negative by use of conventional methods, for example cultures and smear tests. Several studies report the presence of the bacterial ribosomal RNA gene (16S rRNA gene) in ocular fluid from patients with infectious endophthalmitis [2–4]. This broad-range PCR can detect a variety of bacterial DNA by use of primers for conserved regions [5, 6], and the combination of broad-range PCR and quantitative PCR for infectious bacterial endophthalmitis is now available [4]. Real-time PCR enables quantification of bacterial loads in a sample. However, the efficiency of extraction of bacterial DNA from ocular fluid by use of a robotic extraction machine is not yet established. Therefore, establishment of a precise extraction procedure is needed for diagnostic clinical use. In addition, broad-range real-time PCR assays are rarely designed to identify bacterial DNA in clinical samples and are not widely used for ophthalmologic diagnosis.

The objectives of this study using broad-range real-time PCR assays were:

1. to determine optimum methods of DNA extraction;
2. to evaluate the sensitivity of the real-time PCR assay in vitreous samples; and
3. to include and test several main causative agents of infectious bacterial endophthalmitis.

Methods

This study was performed in accordance with the tenets of the Declaration of Helsinki and approved by the Institutional Ethics Committees of Tokyo Medical and Dental University.

Bacterial strains

Reference bacterial strains were provided by the National Institute of Technology and Evaluation (NITE, Tokyo, Japan), the NITE Biological Resource Center (NBRC, Chiba, Japan), the Research Institute for Microbial Diseases (RIMD; Osaka University, Osaka, Japan), and the Japan Collection of Microorganisms (JCM, Saitama, Japan). Frequently reported pathogenic bacteria of endophthalmitis were tested, including 12 Gram-positive strains: *Staphylococcus aureus*, methicillin-resistant *Staphylococcus aureus* (MRSA), *Staphylococcus epidermidis*, *Streptococcus pyogenes*, *Streptococcus sanguinis*, *Streptococcus pneumoniae*, *Enterococcus faecalis*, *Corynebacterium diphtheriae*, *Bacillus cereus*, *Clostridium perfringens*, *Propionibacterium acnes*, and *Nocardia asteroides* and 4 Gram-negative strains: *Escherichia coli*, *Klebsiella pneumoniae*, *Pseudomonas aeruginosa*, and *Moraxella lacunata* [7–14].

Before PCR assay, *S. aureus* and *S. epidermidis* strains were cultured in Trypticase soy broth (Difco; BD Diagnostic Systems, Sparks, MD, USA). *S. pyogenes* and *S. sanguinis* strains were cultured in Todd Hewitt broth (Difco) containing 2 % yeast extract (Difco). *E. coli* and *B. cereus* strains were cultured in LB broth (Nacalai Tesque, Kyoto, Japan). The *K. pneumoniae* strain was cultured in nutrient broth (Difco). All bacterial strains were grown until the mid-log phase at 37 °C. Bacterial cells were washed twice with PBS, and then re-suspended in PBS at appropriate concentrations. The remaining strains were dissolved in physiological salt solution without culture.

DNA extraction

DNA extraction was performed using a DNA extraction card (Qiagen EZ1 Advanced card; Bacteria card® or Virus card®; Qiagen, Valencia, CA, USA) and a DNA Kit (Qiagen DNA tissue kit or Qiagen Virus Mini kit; Qiagen) installed on a robotic workstation set for automated purification of nucleic acids (BioRobot E21, Qiagen). Four extraction procedures were used, as follows:

DNA extraction procedure I	Sample preparation: bacterial culture 180 µl + nuclease-free water 20 µl, and extraction method: Bacteria card® + DNA tissue kit
DNA extraction procedure II	Sample preparation: bacterial culture 180 µl + lysozyme 20 µl (50 mg/ml, Nacalai Tesque), and extraction method: Bacteria card® + DNA tissue kit. Bacterial cultures were pretreated with lysozyme

	and incubated for 30 min at 37 °C
DNA extraction procedure III	Sample preparation: bacterial culture 180 µl + nuclease free water 20 µl, and extraction method: Virus card® + Virus Mini kit
DNA extraction procedure IV	Sample preparation: bacterial culture 180 µl + lysozyme 20 µl (50 mg/ml; incubation for 30 min at 37 °C), and extraction method: Virus card® + Virus Mini kit

After DNA extraction, the DNA concentration was measured by use of the Nano drop 2000 (Thermo Fisher Scientific, Waltham, MA, USA), using between 1 and 10 ng/mL bacterial DNA.

Real-time PCR

The primer pairs and TaqMan probe for conserved bacterial 16S rRNA genes and PCR conditions were as described elsewhere [5]. The sense primer (Bac349F) was 5′-AGG CAGCAGTDRGGAAT-3′, the antisense primer (Bac 806R) was 5′-GGACTACYVGGGTATCTAAT-3′, and the TaqMan probe was 5′-FAM-TGCCAG CAGCCGCGG TAATACRDAG-TAMRA-3′. The products were subjected to 45 cycles of PCR amplification (<500 bp), with cycling conditions set at 95 °C for 10 min, followed by 45 cycles at 95 °C for 15 s and 60 °C for 1 min. The real-time PCR was performed using Amplitaq Gold (Applied Biosystems, Foster City, CA, USA) and the Light Cycler 480 II system (Roche, Rotkreuz, Switzerland). Data analysis was performed by using the program of absolute quantification by the Second Derivative Maximum Method installed in Light Cycler 480 II. Standard curves were constructed from serial tenfold dilutions of linearized plasmid DNA as in our previous report [4].

Sensitivity of real-time PCR assay

After informed consent had been obtained, vitreous fluid was collected from 11 patients who received vitreous surgery for non-infectious eye diseases, for example rhegmatogenous retinal detachment, macular edema by branch retinal vein occlusion, and proliferative diabetic retinopathy,. The vitreous samples were diluted threefold with saline before use as a bacterial dilution. The vitreous fluids were centrifuged at 20,000×*g* for 10 min, then the cell pellets were removed.

To evaluate the sensitivity of the real-time PCR assay, bacterial cell numbers were determined by optical density measurements at 600 nm (OD_{600}) in the mid-log phase, and serial dilutions of bacterial culture were plated on the appropriate agar plates, then colony numbers were determined on agar plates. For example, the cell number of *E. coli* at $OD_{600} = 1.0$ was determined to be 8×10^8 CFU/mL, and the cell number of *S. aureus* at $OD_{600} = 1.0$ was determined to be 4×10^8 CFU/mL.

200 µl of a tenfold dilution series from 2.5×10^7 CFU/mL to 2.5×10^1 CFU/mL of *S. aureus* and *E. coli* bacterial culture were centrifuged at 20,000×*g* for 10 min, and pelleted bacteria samples were re-suspended in the same amount of diluted vitreous samples. The bacterial DNA was extracted from 50 µl, from 200 µl of diluted vitreous sample and bacterial pellet, and 10 µl (equivalent to 10^6 CFU/PCR tube to 10^0 CFU/PCR tube) of 50 µl bacterial DNA was used in PCR reactions. The diluted vitreous samples without bacterial cells were used as a negative control.

Results

Analytical sensitivity of broad-range real-time PCR in relation to the four DNA extraction procedures

Four DNA extraction procedures (I–IV) were compared and analyzed. As described in Table 1, the analytical sensitivity of the broad-range real-time PCR was assessed by use of seven representative bacterial strains including five Gram-positive strains (*S. aureus, S. epidermidis, S. pyogenes, S. sanguinis,* and *B. cereus*) and two Gram-negative strains (*E. coli* and *K. pneumoniae*). For negative control samples levels were undetectable for all extraction methods. DNA extraction using Bacteria card® without enzymes resulted in the detection at concentrations of $\leq 10^7$ copies/mL for all strains. Extraction with the Bacteria card® with lysozyme detected concentrations of $\leq 10^6$ copies/mL, indicating there was no significant difference between the two procedures (Table 1). In contrast, DNA extraction with the Virus card® both with and without enzymes resulted in the detection of 10^4–10^8 copies/mL for all strains, which was much less than the detection obtained with the Bacteria card®. Therefore, procedures using Bacteria card® could be used to treat samples of clinically suspected infectious endophthalmitis. In addition, lysozyme treatment is not needed even for detection of Gram-positive bacteria in ocular samples.

Sensitivity of the PCR assay for vitreous samples

PCR results for the prepared vitreous samples showed sensitivity of detection was highest for *S. aureus* bacterial

Table 1 Summary of the analytical sensitivity of broad-range real-time PCR assays in relation to DNA extraction methods

Strain	Number of bacteria DNA (copies/mL)			
	Procedure I	Procedure II	Procedure III	Procedure IV
Gram-positive strains				
Staphylococcus aureus	10^8	10^7	10^5	10^7
Staphylococcus epidermidis	10^8	10^8	10^8	10^8
Streptococcus pyogenes	10^7	10^8	10^4	10^7
Streptococcus sanguinis	10^7	10^8	10^6	10^8
Bacillus cereus	10^8	10^8	10^7	10^7
Gram-negative strains				
Escherichia coli	10^7	10^6	10^7	10^5
Klebsiella pneumoniae	10^7	10^7	10^5	10^6
Negative control	<10	<10	<10	<10

DNA extraction procedure I: sample: bacterial culture 180 µl + nuclease-free water 20 µl, and extraction method: Bacteria card® + DNA tissue kit. procedure II: sample: bacterial culture 180 µl + lysozyme 20 µl, and extraction method: Bacteria card® + DNA tissue kit. procedure III: Sample: bacterial culture 180 µl + nuclease free water 20 µl, and extraction method: Virus card® + Virus Mini kit. procedure IV: sample: bacterial culture 180 µl + lysozyme 20 µl, and extraction method: Virus card® + Virus Mini kit

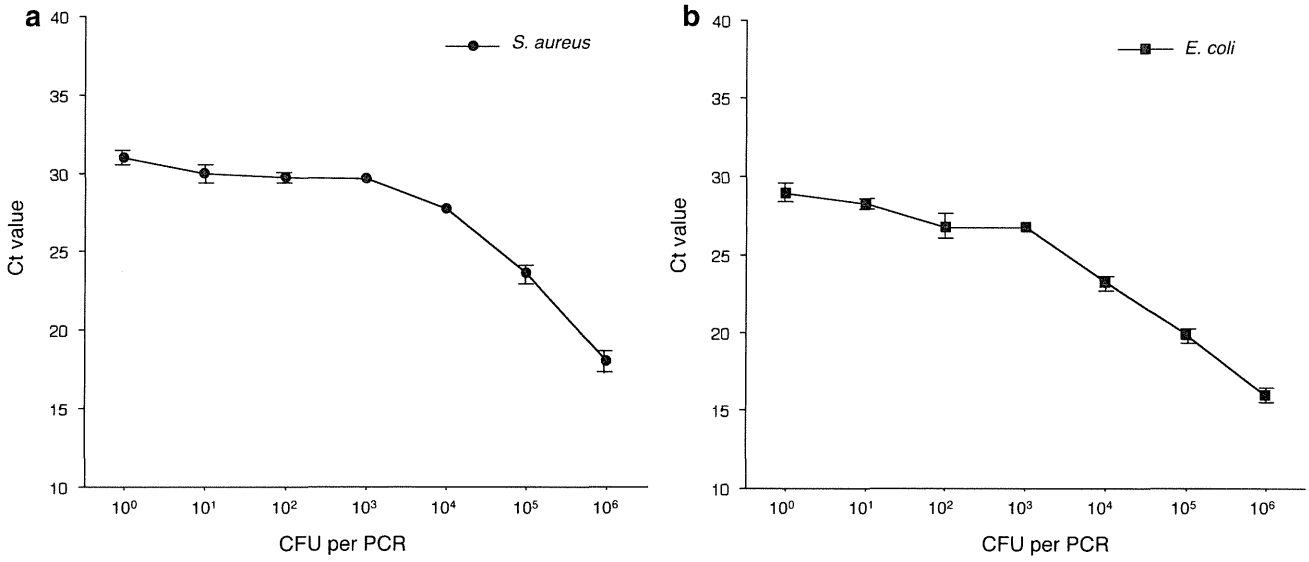

Fig. 1 Analytical detection ranges and sensitivities of a broad-range real-time PCR assay in diluted vitreous samples. **a** Detection of *S. aureus*. **b** Detection of *E. coli*. Results shown are the means and standard deviations of three independent experiments

DNA (concentration $\geq 10^1$ CFU per PCR; Fig. 1a). There was no detection in the negative controls of nuclease-free water. PCR of vitreous sample mixed with *E. coli* resulted in C_t values similar to those for *S. aureus*, i.e., concentration of 10^0 per PCR (Fig. 1b), and there was no detection in the negative controls.

Detection of bacterial DNA of the main causative agents of infectious endophthalmitis by broad-range real-time PCR

For the assay, bacterial DNA was extracted from 200 µl bacterial culture using DNA extraction procedure I. Use of DNA extraction with the Bacteria card® without enzymes and broad-range real-time PCR assay resulted in the detection of concentrations between 5.8×10^3 and 3.5×10^5 copies/mL for all 16 strains. There was no detection in the negative controls of nuclease-free water. Results are shown in Table 2.

Discussion

In this study, we evaluated a broad-range real-time PCR targeting bacterial 16S rRNA genes for detection of bacterial DNA in ocular samples of infectious endophthalmitis.

Table 2 Broad-range real-time PCR detection of bacterial DNA in main causative agents of infectious endophthalmitis

Strain	Clone no.	DNA (ng/mL)	C_t value	Copies/mL
Gram-positive strains				
Staphylococcus aureus	NBRC12732	7.3	28.7	1.3×10^4
MRSA	JCM8702	7.0	29.1	1.0×10^4
Staphylococcus epidermidis	JCM2414	6.0	27.9	1.7×10^4
Streptococcus pyogenes	RIMD 3123004	7.2	28.0	1.6×10^4
Streptococcus sanguinis	JCM5708	3.6	29.1	9.7×10^3
Streptococcus pneumoniae	NBRC102642	8.2	25.7	9.4×10^4
Enterococcus faecalis	JCM20313	2.0	24.0	1.1×10^5
Corynebacterium diphtheriae	JCM1310	4.4	25.2	6.1×10^4
Bacillus cereus	JCM20266	4.9	26.8	2.9×10^4
Clostridium perfringens	JCM1290	6.1	29.9	5.8×10^3
Propionibacterium acnes	JCM6425	1.4	28.3	1.5×10^4
Nocardia asteroides	NBRC14403	8.0	28.7	1.3×10^4
Gram-negative strains				
Escherichia coli	JCM20135	8.7	23.2	1.5×10^5
Klebsiella pneumoniae	JCM1662	7.5	26.8	2.9×10^4
Pseudomonas aeruginosa	JCM6425	5.6	23.7	3.5×10^5
Moraxella lacunata	JCM20914	3.2	25.8	8.9×10^4

Levels were undetectable in the negative control sample (<10 copies/mL) on PCR assay

MRSA methicillin-resistant *Staphylococcus aureus*

Using this broad-range PCR, we are able to measure amplification of the bacteria 16S target ribosomal RNA genes. To detect different bacterial species, we choose the PCR primers and probe which were constructed within the conserved region of bacterial 16s ribosomal RNA. We evaluated four DNA extraction procedures used for broad-range real-time PCR assays in the detection of bacterial DNA. The broad-range real-time PCR described herein detected as few as 1–10 CFU in diluted vitreous per reaction. In addition, the bacterial 16S-specific broad-range real-time PCR assay could detect the presence of 16 causative bacterial species of infectious endophthalmitis. Thus, the broad-range real-time PCR could comprehensively detect the main causative bacteria in suspected infectious endophthalmitis cases.

The appropriate DNA extraction procedure for verification of bacterial infection by PCR is still controversial. Most studies of broad-range real-time PCR for bacterial infection detection have reported use of commercial kits, enzyme treatment, freezing and thawing or boiling, mechanical disruption, or a combination of these methods [6, 15–17]. In general, pretreatment using bactericidal enzyme is needed for bacterial cell-wall destruction, and several investigators report the presence of lysozyme resistance in Gram-negative bacteria species such as *E. coli* [18] and *P. aeruginosa* [18], and Gram-positive bacteria such as *S. pneumonia* [19]. However, this study found no significant difference between use of the Bacteria card® procedure and the Bacteria card® plus lysozyme-pretreatment procedure for extraction of DNA from the samples. The reasons for this are not clear, but it is assumed it may depend on:

1. the kind of enzyme used; and
2. which bacteria species are treated.

Thus, a combination of several enzyme treatments should be tried whenever possible.

Diagnosis of ocular infectious diseases, including bacterial endophthalmitis and other forms of ocular inflammatory diseases, is often difficult because of the difficulty in obtaining results from the small amounts of ocular samples, extracted from aqueous humor and vitreous fluids, available. There are insufficient amounts of the samples to enable PCR testing and additional examination to determine whether the infectious antigens causing the ocular inflammatory diseases are from a bacterial, viral, fungal, or parasitic infection.

In this study, we conducted various DNA extraction procedures to determine the best DNA extraction method. Compared with the use of the Virus card®, DNA extraction using the Bacteria card® had higher detection efficiency for all the representative strains tested. DNA extraction performed with the Virus card® detected bacterial DNA, but was not as efficient for strains that have a thick cell wall and a capsule, for example *S. aureus, S. pyogenes*, and *K. pneumoniae*. Thus, DNA extraction with the Bacteria card® should be considered for detection of clinically suspected intraocular bacterial infection.

The minimum detection limits of our broad-range real-time PCR assay after DNA extraction using the Bacteria

card® without enzymes was between 10^0 and 10^6 CFU per PCR for the bacterial species investigated. The PCR results from the prepared vitreous sample had the best sensitivity for detection of selected bacterial DNA, for example *S. aureus* and *E. coli* at concentrations of $\geq 10^0$–10^1 CFU per PCR. Zucol et al. [6] report that the sensitivity of their broad-range real-time PCR assay targeting the bacterial 16S rRNA gene was a concentration of $\geq 10^3$ CFU per PCR for detection of *S. aureus* and a concentration of $\geq 10^2$ CFU per PCR for detection of *E. coli*. In addition, the minimum detection limits for *S. aureus* and *E. coli* were determined to be in the range 10–10^3 CFU or CFU equivalents per PCR. Thus, the minimum detection limit of our PCR assay is among the lowest reported so far for these two bacterial species.

In a previous report by Vollmer et al. [20], serum and urine samples were shown to have at least an equal effect on the Ct values, whereas blood and tracheal secretion samples had stronger effects. They suggest that the delayed C_t values of blood sample (EDTA-anti-coagulated) are mainly affected by background human DNA, whereas the viscous character of samples primarily affected the C_t values of tracheal secretion samples. Because our vitreous samples included less human DNA and the diluted sample was actually non-viscous, detection of bacterial DNA from prepared vitreous samples was shown to be highly sensitive.

Recently, we reported that broad-range real-time PCR of the bacterial 16S rRNA gene is a useful tool for clinically diagnosing suspected bacterial endophthalmitis [4]. In an earlier clinical study, we successfully detected bacterial 16S DNA in all cases of bacterial endophthalmitis ($n = 18$), with the exception of one patient. The single PCR-negative patient was suspected of having infectious endophthalmitis but had no bacteria in his ocular sample; *K. pneumoniae* was detected by biopsy culture of liver infection. However, as described in this study, our bacterial 16S-specific broad-range real-time PCR can detect candidate bacterial DNA including *K. pneumoniae* (Table 2). *K. pneumoniae* is a common cause of endogenous infectious endophthalmitis, a disease that frequently results in poor vision. *K. pneumoniae* endophthalmitis is strongly associated with the presence of liver abscesses and an underlying diabetic condition. We collected aqueous humor samples from the patient after informed consent had been obtained. Had a vitreous sample also been obtained, we might have been able to detect the bacterial DNA, because *K. pneumoniae*-associated endophthalmitis often results from hematogenous dissemination. To make an accurate diagnosis, sample preparation of clinical specimens is very important. A vitreous or retinal biopsy sample should be collected in such cases because inflammation often occurs in the subretinal area around the choroid because of endogenous infections.

In conclusion, we were able to use a broad-range real-time PCR method to measure the amplification of target ribosomal RNA genes, for example the bacterial 16S rRNA gene, indicating the suitability of this assay for screening for increased levels of bacterial genes in samples. Importantly, these PCR assays may be used for detection of candidate bacterial species that cause infectious endophthalmitis. The detection limit of our real-time PCR assay is one 16S rRNA gene copy per PCR. Thus, this PCR assay enables rapid screening for bacterial infection in a variety of clinical specimens from the eye.

Acknowledgments The authors thank Ikuyo Yamamoto, Shizu Inoue, and Chizuru Kato for providing technical assistance and the doctors of the Uveitis Group at Tokyo Medical and Dental University Hospital for sample collection. This work was supported by the Comprehensive Research on Disability, Health and Welfare, Health and Labor Sciences Research Grants, Ministry of Health, Labor and Welfare, Japan.

References

1. Brun-Buisson C, Fartoukh M, Lechapt E, Honoré S, Zahar JR, Cerf C, et al. Contribution of blinded, protected quantitative specimens to the diagnostic and therapeutic management of ventilator-associated pneumonia. Chest. 2005;128:533–44.
2. Therese KL, Anand AR, Madhavan HN. Polymerase chain reaction in the diagnosis of bacterial endophthalmitis. Br J Ophthalmol. 1998;82:1078–82.
3. Chiquet C, Cornut PL, Benito Y, Thuret G, Maurin M, Lafontaine PO, et al. Eubacterial PCR for bacterial detection and identification in 100 acute postcataract surgery endophthalmitis. Invest Ophthalmol Vis Sci. 2008;49:1971–8.
4. Sugita S, Shimizu N, Watanabe K, Katayama M, Horie S, Ogawa M, et al. Diagnosis of bacterial endophthalmitis by broad-range quantitative PCR. Br J Ophthalmol. 2011;95:345–9.
5. Takai K, Horikoshi K. Rapid detection and quantification of members of the archaeal community by quantitative PCR using fluorogenic probes. Appl Environ Microbiol. 2000;66:5066–72.
6. Zucol F, Ammann RA, Berger C, Aebi C, Altwegg M, Niggli FK, et al. Real-time quantitative broad-range PCR assay for detection of the 16S rRNA gene followed by sequencing for species identification. J Clin Microbiol. 2006;44:2750–9.
7. Usui N, Uno T, Oki K, Oshika T, Ohashi Y, Ogura Y, et al. Nationwide surveillance of postoperative endophthalmitis related to cataract surgery. Jpn J Ophthalmic Surg. 2006;19:73–9.
8. Aaberg TM Jr, Flynn HW Jr, Schiffman J, Newton J. Nosocomial acute-onset postoperative endophthalmitis survey. A 10-year review of incidence and outcomes. Ophthalmology. 1998;105:1004–10.
9. Vafidis G. Propionibacterium acnes endophthalmitis. Br J Ophthalmol. 1991;75:706.
10. Boldt HC, Pulido JS, Blodi CF, Folk JC. Rural endophthalmitis. Ophthalmology. 1989;96:1722–6.
11. Jackson TL, Eykyn SJ, Graham EM, Stanford MR. Endogenous bacterial endophthalmitis: a 17-year prospective series and review of 267 reported cases. Surv Ophthalmol. 2003;48:403–23.
12. Chen YJ, Kuo HK, Wu PC, Kuo ML, Tsai HH, Liu CC, et al. A 10-year comparison of endogenous endophthalmitis outcomes: an east Asian experience with *Klebsiella pneumoniae* infection. Retina. 2004;24:383–90.

13. Callegan MC, Engelbert M, Parke DW 2nd, Jett BD, Gilmore MS. Bacterial endophthalmitis: epidemiology, therapeutics, and bacterium–host interactions. Clin Microbiol Rev. 2002;15: 111–24.
14. Callegan MC, Gilmore MS, Gregory M, Ramadan RT, Wiskur BJ, Moyer AL, et al. Bacterial endophthalmitis: therapeutic challenges and host–pathogen interactions. Prog Retin Eye Res. 2007;26:189–203.
15. Tomaso H, Kattar M, Eickhoff M, Wernery U, Al Dahouk S, Straube E, et al. Comparison of commercial DNA preparation kits for the detection of Brucellae in tissue using quantitative real-time PCR. BMC Infect Dis. 2010;10:100.
16. Tsai YL, Olson BH. Rapid method for direct extraction of DNA from soil and sediments. Appl Environ Microbiol. 1991;57: 1070–4.
17. Lee YK, Kim HW, Liu CL, Lee HK. A simple method for DNA extraction from marine bacteria that produce extracellular materials. J Microbiol Methods. 2003;52:245–50.
18. Callewaert L, Aertsen A, Deckers D, Vanoirbeek KG, Vanderkelen L, Van Herreweghe JM, et al. A new family of lysozyme inhibitors contributing to lysozyme tolerance in gram-negative bacteria. PLoS Pathog. 2008;4:e1000019. doi:10.1371/journal.ppat.1000019.
19. Davis KM, Akinbi HT, Standish AJ, Weiser JN. Resistance to mucosal lysozyme compensates for the fitness deficit of peptidoglycan modifications by *Streptococcus pneumoniae*. PLoS Pathog. 2008;4:e1000241. doi:10.1371/journal.ppat.1000241.
20. Vollmer T, Störmer M, Kleesiek K, Dreier J. Evaluation of novel broad-range real-time PCR assay for rapid detection of human pathogenic fungi in various clinical specimens. J Clin Microbiol. 2008;46:1919–26.

Virological Analysis in Patients with Human Herpes Virus 6–Associated Ocular Inflammatory Disorders

Sunao Sugita,[1,2] *Norio Shimizu,*[3] *Ken Watanabe,*[3] *Manabu Ogawa,*[2] *Kazuichi Maruyama,*[4] *Norio Usui,*[5] *and Manabu Mochizuki*[2]

Purpose. To determine whether human herpes virus 6 (HHV-6) genomic DNA and mRNA can be detected in ocular samples from patients with inflammatory disorders, and whether viral replication is involved in the development of inflammation in the eye.

Methods. After informed consent was obtained, ocular fluid samples (aqueous humor and vitreous fluids) were collected from 350 patients with uveitis or endophthalmitis. Corneal samples were also collected from 65 patients with corneal infections. Multiplex PCR was performed to screen ocular samples from the patients for HHV-1 to HHV-8. Samples were also assayed for HHV-6 DNA using quantitative real-time PCR. Primers for nested RT-PCR were designed to detect amplification of mRNA (HHV-6 A IE1 U90).

Results. PCR results indicated a total of seven patients with uveitis or endophthalmitis (7/350, 2% +) and a single patient with corneal inflammatory disease were positive for HHV-6 DNA (1/65, 1.5% +). These eight patients had high copy numbers of HHV-6 DNA, with values ranging from 4.0×10^3 to 5.1×10^6 copies/mL. Real-time PCR analysis indicated that two of these cases were HHV-6 variant A and six cases were variant B. In addition, HHV-6 mRNA was clearly detected in vitreous cells collected from one of the patients, suggesting that viral replication may occur in the eye.

Conclusions. Our results indicate that HHV-6 infection/reactivation is implicated in ocular inflammatory diseases. (www.umin.ac.jp/ctr/index/htm number, R000002708.) (*Invest Ophthalmol Vis Sci.* 2012;53:4692–4698) DOI:10.1167/iovs.12-10095

Human herpesvirus 6 (HHV-6) is the causative agent of exanthema subitum in children and has been associated with a number of inflammatory and neurological disorders worldwide. It has been implicated in hepatitis, pneumonitis, and severe infections of the central nervous system in both immunosuppressed and immunocompetent patients. HHV-6 can reactivate from its latent form after primary infection. In the case of eye diseases, it has been implicated in AIDS-associated retinitis,[1–3] uveitis,[4–8] corneal inflammation,[9] and optic neuropathy.[10–12] Two variants of HHV-6 have been identified. HHV-6A is less often associated with disease and has a greater predilection for neural cells than HHV-6B.[13] Although HHV-6A DNA is frequently found in the nervous system of infected adults, HHV-6B DNA is rarely present in ocular fluids, although it is found in most documented primary HHV-6 infections.

Diagnosis of clinically relevant HHV-6 can be challenging due to the high prevalence of infection and viral persistence. Detection of viral nucleic acids may indicate active or latent infections, depending on the clinical setting and specimens tested. Quantitative PCR methods have been established to detect active infections. Detection of HHV-6 DNA in plasma or serum is indicative of active replication and is therefore more directly interpretable.[14,15] Using these PCR techniques, several investigators previously reported that HHV-6 genomic DNA is found in ocular inflammatory diseases, including infectious uveitis and endophthalmitis[1–8]; however, involvement of HHV-6 in ocular infections has not yet been clearly demonstrated.

Therefore, we designed experiments to investigate whether ocular samples from patients with various ocular inflammatory disorders contain HHV-6 genomic DNA, whether ocular samples from noninflammatory patients also contain HHV-6 DNA, whether positive cases are either HHV-6 variant A or B, and whether HHV-6 mRNA as well as a high copy numbers of HHV-6 DNA can be detected in positive samples.

Materials and Methods

Subjects

The first patient group was examined between 2006 and 2010 at the Tokyo Medical and Dental University Hospital, Kyoto Prefectural University Hospital, and Shinkawabashi Hospital in Japan. After informed consent was obtained, ocular fluid samples were collected from patients with uveitis (infectious and noninfectious) or endophthalmitis. This group included consecutive patients with uveitis or endophthalmitis (n = 350), including a previously HHV-6–positive severe panuveitis case.[7] Corneal tissues were also collected from patients with ocular surface diseases (e.g., keratitis, n = 65). At this time, we excluded ocular tumor diseases (e.g., intraocular lymphoma) from the patient group.

In addition to the patient group, we also analyzed samples from a control group. A total of 100 samples (50 aqueous humor and 50 vitreous fluids) were collected from patients who did not have any type of ocular inflammation (age-related cataract, macular edema, retinal

From the [1]Laboratory for Retinal Regeneration, RIKEN Center for Developmental Biology, Kobe, Japan; Departments of [2]Ophthalmology & Visual Science and [3]Virology, Medical Research Institute, Tokyo Medical and Dental University Graduate School of Medicine and Dental Sciences, Tokyo, Japan; [4]Department of Ophthalmology, Kyoto Prefectural University of Medicine, Kyoto, Japan; and [5]Department of Ophthalmology, Shinkawabashi Hospital, Kanagawa, Japan.

Supported by Comprehensive Research on Disability, Health and Welfare, Health and Labour Sciences Research Grants, Ministry of Health, Labour, and Welfare, Japan.

Submitted for publication April 26, 2012; revised May 29, 2012; accepted June 10, 2012.

Disclosure: **S. Sugita**, None; **N. Shimizu**, None; **K. Watanabe**, None; **M. Ogawa**, None; **K. Maruyama**, None; **N. Usui**, None; **M. Mochizuki**, None

Corresponding author: Sunao Sugita, Laboratory for Retinal Regeneration, RIKEN Center for Developmental Biology, 2-2-3 Minatojima-minamimachi, Chuo-ku, Kobe 650-0047, Japan; sunaoph@cdb.riken.jp.

Investigative Ophthalmology & Visual Science, July 2012, Vol. 53, No. 8

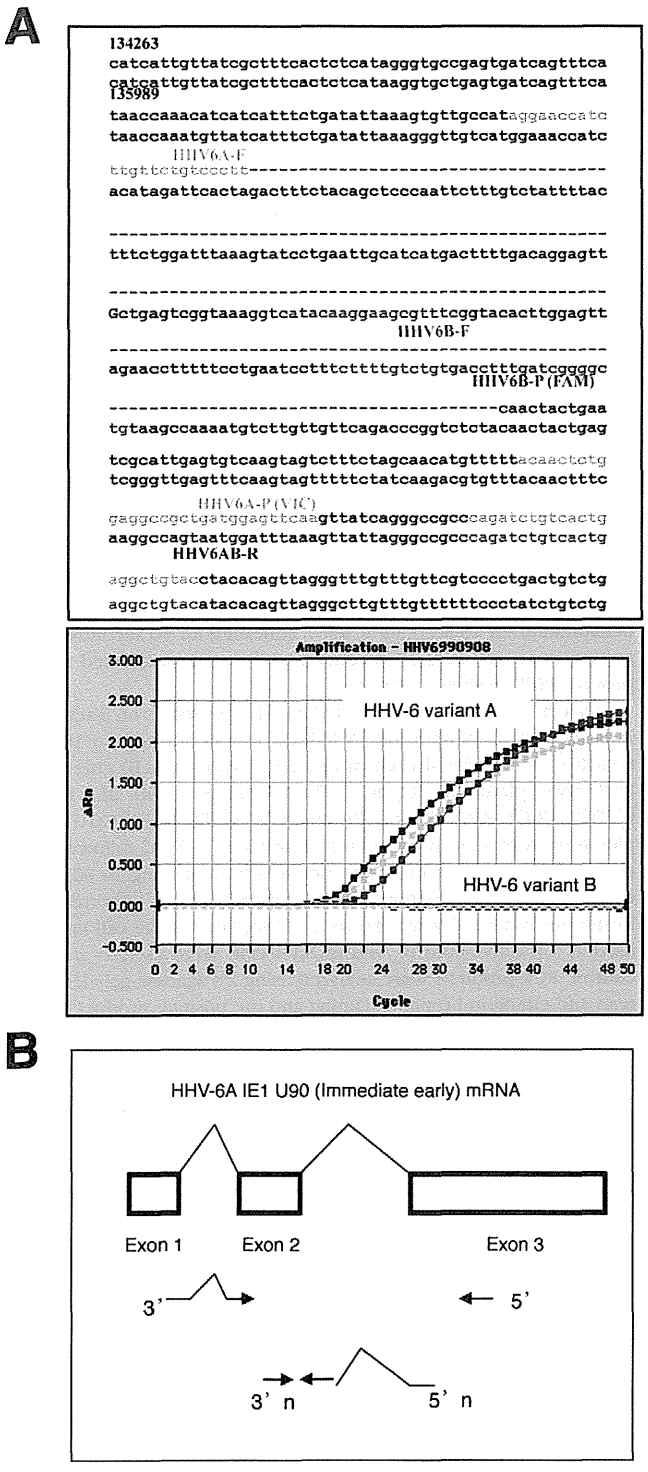

Figure 1. Amplification of HHV-6-specific DNA and mRNA. **(A)** TaqMan probes and primers used to amplify HHV-6 DNA (HHV-6A and HHV-6B). HHV-6 subtypes were identified using PCR with variant-specific primers and probes (*lower graph*). **(B)** Nested RT-PCR primers were designed to amplify HHV-6A mRNA.

detachment, idiopathic macular hole, or idiopathic epiretinal membrane).

The research followed the tenets of the Declaration of Helsinki and all study protocols were approved by the Institutional Ethics Committee of Tokyo Medical and Dental University. A clinical trial registration was conducted and information is available at www.umin.

Table 1. Clinical Findings in Patients with HHV-6–Associated Ocular Inflammatory Disorders

Case	Age / Sex	Eye	Initial Diagnosis	VA	IOP	Cornea	AC	KPs	VO	Fundus	Bacterial Examination*	Final Diagnosis
1	75 / Male	R	Pan-uveitis	0.02	15	None	Hypopyon	Mutton fat	Grade III	Retinal exudates	Culture (-) / PCR (-)	Ocular toxocariasis
2	64 / Female	L	Corneal endotheliitis	0.5	33	Edema	Cell 2+	Mutton fat	None	None	PCR (-)	HSV-1 corneal endotheliitis
3	70 / Male	L	Bacterial endophthalmitis	sl-	35	None	Hypopyon	Fine	Grade III	Retinal necrosis	Culture (+) / PCR (+)	Endogenous endophthalmitis
4	74 / Female	R	Idiopathic uveitis	0.8	16	None	Cell1+	None	Grade II	None	PCR (+)	Late postoperative endophthalmitis
5	79 / Female	L	Bacterial endophthalmitis	mm	19	None	Hypopyon	Fine	Grade II	Retinal exudates, hemorrhage	Culture (+) / PCR (+)	Acute postoperative endophthalmitis
6	71 / Female	L	Necrotic retinitis	0.04	12	None	None	None	None	Retinal necrosis, hemorrhage	PCR (-)	Cytomegalovirus retinitis
7	24 / Female	L	Posner-Schlossman synd.	1.2	24	None	Cell 1+	Mutton fat	None	None	PCR (-)	Idiopathic uveitis
8	22 / Male	R	Karatitis	0.7	15	Infiltration	Cell1-	None	None	None	Culture (-) / PCR (+)	Bacterial karatitis

* Bacterial examination: Results for bacterial culture and/or PCR (bacterial 16S rDNA).
AC, anterior chamber; KPs, keratic precipitates; VA, visual acuity by Landolt Chart; VO, vitreous opacity.

TABLE 2. Virological Analysis and Treatment in Patients with HHV-6-Associated Ocular Inflammatory Disorders

Case	Ocular Sample	HHV Genome	Viral Copy No. by Real-Time PCR	HHV-6A or B	Treatment
1	Aqh	HHV-6	HHV-6: 2.4×10^6 copies/mL	HHV-6A	PSL, PPV, VCV, VGV
	VF	HHV-6, EBV	HHV-6: 2.0×10^4copies/mL, EBV: <50 copies/mL		
2	Aqh	HHV-6, HSV-1	HHV-6: 7.5×10^3copies/mL, HSV-1: 2.8×10^5 copies/mL	HHV-6B	VGV
3	VF	HHV-6	HHV-6: 5.1×10^6 copies/mL	HHV-6B	PPV, SA, IAI
4	VF	HHV-6	HHV-6: 1.1×10^4 copies/mL	HHV-6B	PPV, VGV
5	VF	HHV-6	HHV-6: 1.1×10^6 copies/mL	HHV-6B	PPV, SA, Betametasone
6	VF	HHV-6, CMV	HHV-6: 4.4×10^4 copies/mL, CMV: 1.6×10^6 copies/mL	HHV-6A	VGV
7	Aqh	HHV-6	HHV-6: 4.0×10^3 copies/mL	HHV-6B	None
8	Cornea	HHV-6	HHV-6: 3.9×10^6 copies/μg · DNA	HHV-6B	Antibiotics

Aqh, aqueous humor; IAI, intravitreal antibiotic injection; PPV, pars plana vitrectomy; PSL, prednisolone; SA, systemic antibitotics; VCV, valacyclovir; VF, vitreous fluids; VGV, valganciclovir.

ac.jp/ctr/index/htm with study number of R000002708. The study started in April 2006 and terminated in April 2010.

PCR

DNA was extracted from samples using an E21 virus minikit (Qiagen, Valencia, CA) installed on a robotic workstation for automated purification of nucleic acids (BioRobot E21, Qiagen). HHV genomic DNA in ocular samples was detected using two independent PCR assays: a qualitative multiplex PCR and a quantitative real-time PCR.[16]

The multiplex PCR was designed to qualitatively measure genomic DNA of eight human herpes viruses as follows: herpes simplex virus type 1 (HSV-1), type 2 (HSV-2), Varicella-zoster virus (VZV), Epstein-Barr virus (EBV), cytomegalovirus (CMV), and human herpes virus 6 (HHV-6), 7 (HHV-7), and 8 (HHV-8). PCR was performed using a LightCycler (Roche, Rotkrevz, Switzerland). Primers for HHV-6 were as follows: Forward - ACCCGAGAGATGATTTTGCG and Reverse - GCAGAAGA-CAGCAGCGAGAT. Probes were used as follows: 3'FITC-TAAG-TAACCGTTTTCGTCCCA and LcRed705-5'-GGGTCATTTATGTTATAGA. These primers and probes do not distinguish between HHV-6A and B. PCR conditions, primers, and probes specific for other HHV have been described previously.[17]

Real-time PCR was performed for detection of HHV only, following identification of genomic DNA by multiplex PCR. Real-time PCR was performed using Amplitaq Gold and the Real-Time PCR 7300 system (ABI, Foster City, CA). The sequence of the HHV-6 primers and probes are as follows: Forward - GACAATCACATGCCTGGATAATG and Reverse - TGTAAGCGTGTGGTAATGTACTAA. The probe was AG-CAGCTGGCGAAAAGTGCTGTGC. The primers and probes of other herpes viruses and the PCR conditions have been described previously.[16,17] These primers and probes do not distinguish between HHV-6A and B. TaqMan probes and primers used in the HHV-6 DNA amplifications, HHV-6 type A and HHV-6 type B, are shown in Figure 1A. The value of viral copy number in the sample was considered to be significant when more than 50 copies/mL were observed.

RT-PCR

The primers for nested RT-PCR were designed to detect mRNA (HHV-6 A IE1 U90 immediate early) as follows: first PCR Forward - GATGAACGTATGCAAGACTACC and ATGAACATGGATTGTTGCTG and Reverse - CAGCGGACTGAGCAGCTA; nested PCR Forward - CCGATCCAATGATGGAAGAA and Reverse - CAGCGGACTGAGCAGC-TA (Fig. 1B). A one-step RT-PCR was performed on 100 ng of total RNA with 0.5 μM of each primer and SuperScript III One-Step RT-PCR with platinum Taq (Life Technologies Co., Tokyo, Japan) in a final volume of 50 μL. Samples were reverse transcribed for 30 minutes at 54°C and amplified for 40 cycles consisting of denaturation for 15 seconds at 94°C, annealing for 30 seconds at 54°C, and polymerization for 20 seconds at 72°C. Following identification of a PCR product of 340 bp, nested PCR was performed on 1 μL of the first PCR solution using 0.5 μM of each primer and 200 mM deoxynucleotide triphosphates and 1.25 U of Taq DNA polymerase (Thermo Fisher Scientific, Tokyo, Japan). Monoclonal antibody (anti-taq high: Toyobo Life Science, Tokyo, Japan) was used at 0.25 μg in a buffer containing 75 mM Tris-HCl (pH = 8.8), 0.01% Tween-20, 20 mM $(NH_4)_2SO_4$, and 1.5 mM $MgCl_2$ in a final volume of 50 μL. Twenty cycles of amplification consisting of denaturation for 15 seconds at 94°C, annealing for 30 seconds at 55°C, and polymerization for 15 seconds at 72°C were performed to give a positive PCR product of 198 bp.

All ocular samples were tested for the presence of β-actin as an internal control. β-Actin mRNA RT-PCR was performed on 100 ng of total RNA with 0.5 μM each primer and SuperScript III One-Step RT-PCR with platinum Taq in a final volume of 50 μL (Forward-CTTCCTTCCTGGGCAT and Reverse-TCTTCATTGTGCTGGGT). Samples were reverse transcribed for 30 minutes at 55°C followed by 40 cycles of denaturation for 30 seconds at 94°C, annealing for 30 seconds at 60°C, and polymerization for 1 minute at 72°C on a thermal cycler TP-400 instrument (Takara Bio Inc., Tokyo, Japan). Raji cell lines were used as a positive control, and MOLT-4 cells were used as a negative control. PCR products were analyzed using 2% agarose gel electrophoresis and ethidium bromide staining and the positive product was 215 bp.

RESULTS

Detection of HHV-6 Genomic DNA in Patients with Uveitis, Endophthalmitis, and Ocular Surface Diseases

We first performed multiplex PCR to screen for 8 HHVs after collecting intraocular samples from patients with various ocular inflammatory diseases. PCR results indicated that 7 (2%) of 350 patients with uveitis or endophthalmitis were positive for HHV-6 DNA. In addition, 1 (1.5%) of 65 patients tested positive for HHV-6 in a corneal tissue sample. These HHV-6-positive cases together with clinical findings are summarized in Tables 1 and 2. These eight HHV-6-positive patients were clinically suspected to have HHV-6-associated infectious diseases based on the detection of HHV-6 genome in ocular fluid or corneal tissue samples. HHV-6 DNA was not detected in any of the 100 control samples that were collected from patients without ocular inflammation.

The clinical features observed in HHV-6-positive cases at their initial presentation are summarized in Table 1. Almost all of the patients with uveitis and endophthalmitis had active ocular inflammation, that is, there were anterior chamber cells (except case 6), keratic precipitates (except cases 4 and 6), vitreous opacity (except cases 2 and 7), and fresh retinal exudates/necrosis (except cases 2, 4, and 7). In the single patient with HHV-6^+ keratitis (case 8 in Table 1), corneal

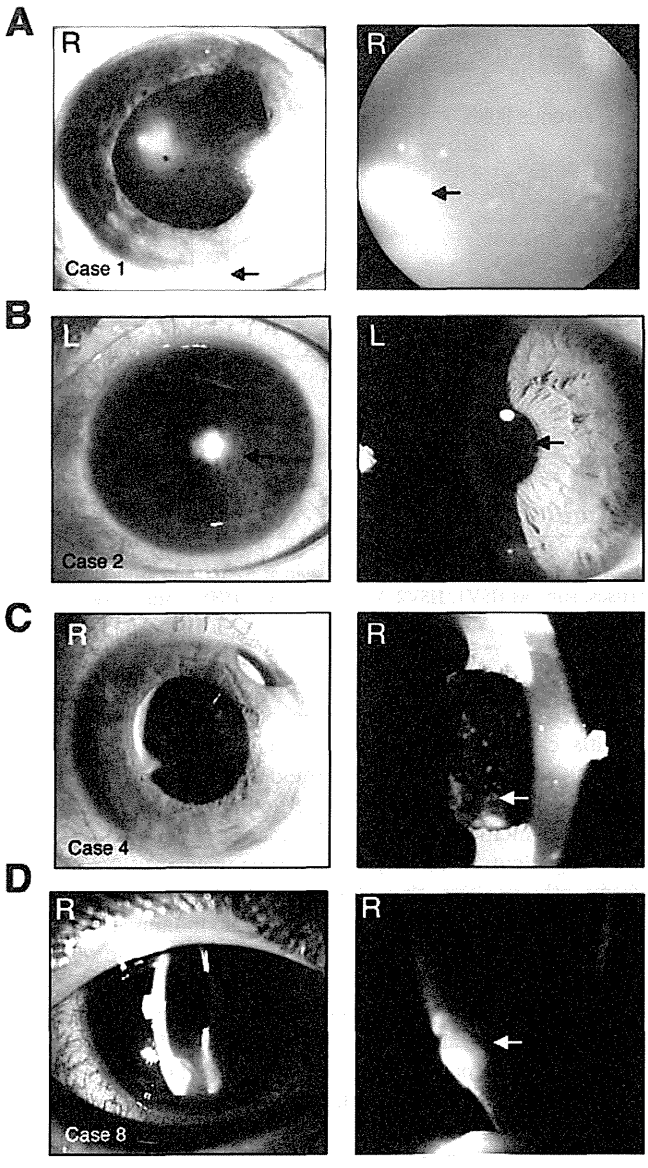

FIGURE 2. Slit-lamp and fundus photographs for HHV-6 infections. (A) Case 1: A case of ocular toxocariasis. Slit-lamp examination of right eye (RE) disclosed ciliary injection, moderate mutton-fat keratic precipitates (KPs), and severe anterior chamber cells with hypopyon (*arrow*). Funduscopic examination of the RE revealed dense vitreous opacities and yellowish white massive retinal lesions (*arrow*) in the peripheral fundus. HHV-6 DNA was detected in both aqueous humor and vitreous samples. (B) Case 2: A case of HSV-1-associated corneal endotheliitis. Slit-lamp examination of left eye (LE) disclosed pigmented mutton-fat-like KPs with high intraocular pressure, mild anterior chamber cells, and small-size corneal stromal edema (*arrow*). HSV-1 and HHV-6 DNA were detected in aqueous humor, but other HHV-DNA, such as VZV and CMV, was not detected. (C) Case 4: A case of late postoperative endophthalmitis. This patient with Vogt-Koyanagi-Harada disease had postcataract surgery 6 months earlier. Slit-lamp examination of RE disclosed ciliary injection and mild anterior chamber cells. White plaque (*arrow*) on the intraocular lens and mild inflammation were seen, and an aqueous humor sample was obtained. HHV-6 DNA and *Propionibacterium acnes* DNA were detected in the aqueous humor sample. The final diagnosis was *P. acnes*-associated late postoperative endophthalmitis. (D) Case 8: A case of bacterial keratitis. Slit-lamp examination of RE disclosed keratitis (*arrow*) with ciliary injection. A corneal infiltration with epithelial defect was observed and a high copy number of HHV-6 DNA was detected in corneal tissue samples.

infection, such as corneal epithelial ulcer and ciliary injection, was indicated. Representative findings including slit-lamp or fundus photographs for HHV-6-positive cases are shown in Figure 2. In addition, ocular samples from all patients were subjected to bacterial examinations, including conventional bacterial culture and bacterial broad-range PCR (bacterial 16S rDNA)[18] (Table 1). The final diagnoses were as follows: case 1, ocular toxocariasis; case 2, HSV-1 corneal endotheliitis; case 3, endogenous endophthalmitis; case 4, late postoperative endophthalmitis; case 5, acute postoperative endophthalmitis; case 6, CMV retinitis; case 7, idiopathic uveitis; case 8, bacterial keratitis (Table 1).

We next summarized the virological analysis of ocular samples from these eight HHV-6-positive patients (3 aqueous humor, 5 vitreous fluids, and 1 corneal tissue) in Table 2. Multiplex PCR was used to detect HHV infection (HSV-1, HSV-2, VZV, EBV, CMV, HHV-6, HHV-7, and HHV-8). HHV-6 was found together with EBV (only case 1), HSV-1 (only case 2), or CMV (only case 6). Figure 3 is representative of the results of the multiplex PCR where HHV-6 DNA was detected in aqueous and vitreous fluid from case 1. HHV DNA in nine ocular samples from eight cases was also measured by real-time PCR. These patients had high copy numbers of HHV-6 DNA, with values ranging from 4.0×10^3 to 5.1×10^6 copies/mL (Table 2), suggesting that viral replication may occur in the eye. Following diagnosis, 4 patients received antiviral treatment (i.e., valacyclovir or valganciclovir), which controlled their ocular inflammation (Table 2).

Detection of HHV-6 Variant A or B in Patients with HHV-6–Associated Ocular Inflammatory Disorders

HHV-6 can be classified into two groups: a variant A (HHV-6A) and a variant B (HHV-6B).[13] Distinguishing between HHV-6 subtypes is mainly accomplished using PCR techniques, including melting curve[19] or variant-specific primers.[20] Therefore, we next determined whether the HHV-6-positive cases were HHV-6A or B using real-time PCR. In this study, we designed a probe and primers for use in the HHV-6 DNA amplification. The paired primers and TaqMan probes used for detection of HHV-6A and HHV-6B are shown in Figure 1A. By using several different primers and probes, we were able to detect each of these HHV-6 types separately (Fig. 1A). The PCR results from case 1 showed that intraocular samples included HHV-6A but not HHV-6B DNA (Fig. 4). Final analysis with quantitative PCR indicated that two of the cases were positive for HHV-6A and six cases were positive for HHV-6B (Table 2).

Detection of HHV-6 mRNA in Intraocular Samples

RT-PCR has previously been used on mRNA from peripheral blood mononuclear cells to detect actively replicating virus.[21] We therefore tested ocular samples for the presence of HHV-6 mRNA. Various samples, such as aqueous humor, vitreous fluid, retinal membrane tissues, and collected vitreous cells from an HHV-6A-positive case (case 1), were available for the RT-PCR assay. We designed primers to amplify mRNA using a nested RT-PCR (HHV-6 A IE1 U90, Fig. 1B). As revealed in Figure 5, HHV-6A mRNA was clearly detected in vitreous cell samples, but other ocular samples from the same patient were all negative.

DISCUSSION

In this study, we demonstrate that seven patients with uveitis or endophthalmitis were positive for HHV-6 DNA. In addition, one patient with infectious keratitis was also found to be HHV-6-positive. These patients had high copy numbers of HHV-6

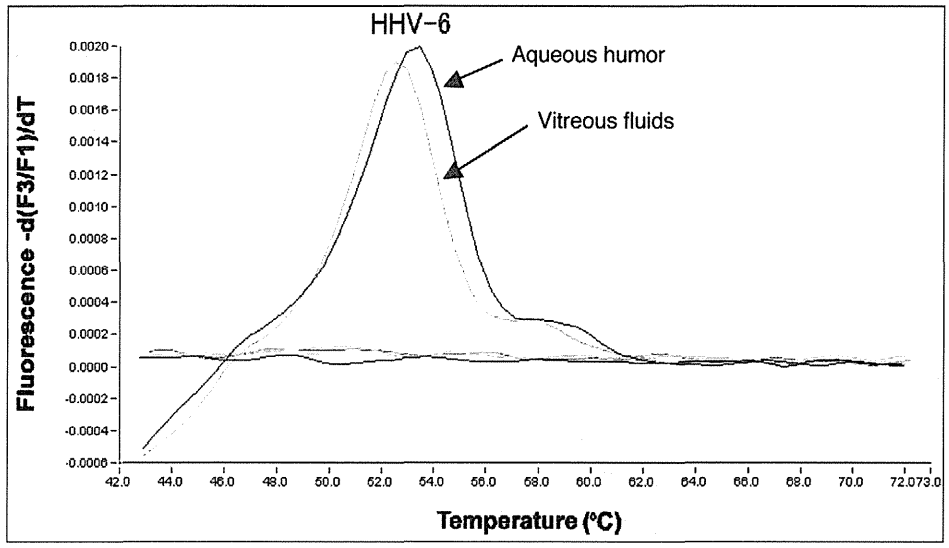

FIGURE 3. Results for multiplex PCR in a patient with HHV-6-positive uveitis. A significant positive curve was seen at 52°C, indicating detection of HHV-6 genomic DNA in the ocular fluids (case 1). DNA from other herpes viruses, such as HSV1, HSV2, VZV, EBV, CMV, HHV7, and HHV8, was not detected in this sample.

DNA, and two cases were found to be HHV-6 type A and six cases were type B. In addition, HHV-6 mRNA was detected in intraocular samples from HHV-6-positive patients, suggesting that viral replication or reactivation may occur in the eye.

Recently, Cohen et al.[5] reported that HHV-6A DNA could be detected by PCR in vitreous fluid from a patient with CMV-associated retinitis when vitreous fluids were assayed from 101 patients with ocular inflammation for HHV-6A, HHV-6B, and HHV-7. HHV-6B DNA was also detected in vitreous fluid from a patient with idiopathic uveitis in the absence of CMV DNA. This study suggests that HHV-6A and HHV-6B DNA are detectable in approximately 1% of vitreous samples from patients with ocular inflammation. In our study, we show that HHV-6 DNA was detectable in 2% of ocular samples from patients with intraocular inflammation following screening for HHV-1 to -8 infection using multiplex PCR.

In a previous study,[16] we found that intraocular HHV DNA was detectable in a wide range of herpes virus-associated uveitis cases when analysis was performed using multiplex PCR. PCR is a valuable tool for the diagnosis of herpetic uveitis and it is now possible to exclude nonherpetic uveitis patients using this method. Moreover, de Boer et al.[8] previously found that in patients with herpetic anterior uveitis, PCR was more frequently positive than the Goldmann-Witmer coefficient. HHV-6 has been implicated in ocular inflammation, most remarkably when the posterior segment of the eye was affected.[6,7,10-12] On the other hand, the role of HHV-6 as a cause of anterior uveitis is inconclusive and further studies are required. As revealed in this study, we found three cases of anterior inflammatory diseases including keratitis and five cases of pan- or posterior inflammatory diseases in the eye.

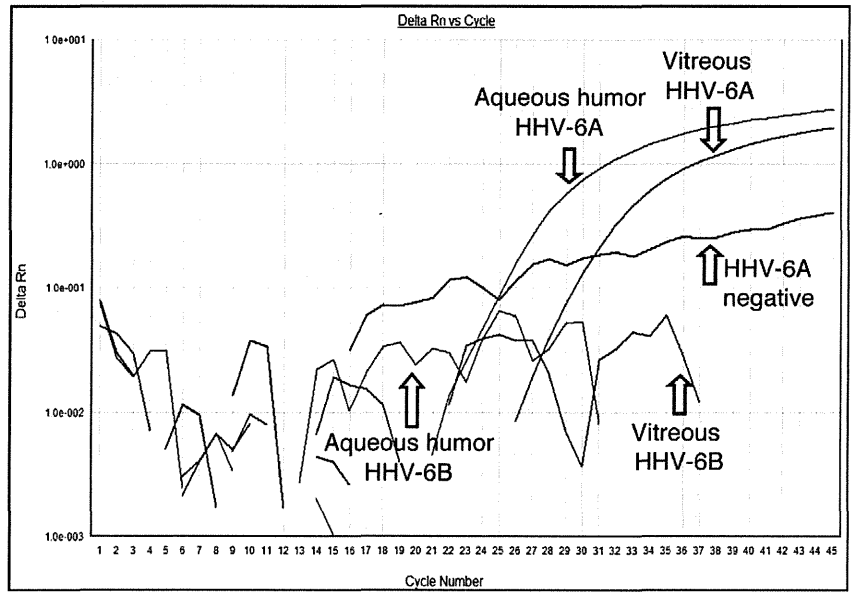

FIGURE 4. Detection of HHV-6 DNA by quantitative real-time PCR. The real-time PCR results for the samples from case 1 showed that intraocular samples, such as aqueous humor and vitreous fluids, contained a high copy number of HHV-6A DNA, but not HHV-6B DNA.

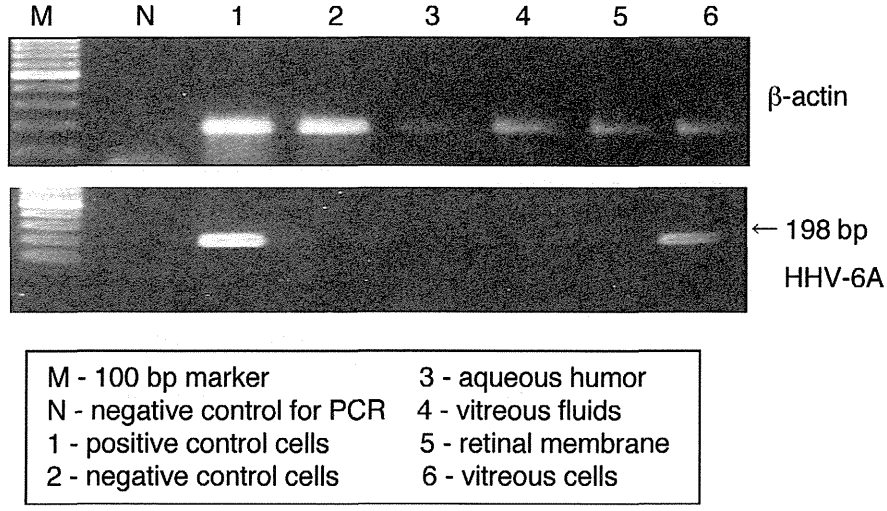

FIGURE 5. Detection of HHV-6 mRNA in intraocular samples. HHV-6A mRNA was detected in samples from vitreous cells, but other ocular samples, such as aqueous humor, vitreous fluids, and retinal membrane tissues were all negative (*lower image*). All samples, including control RNA, were positive for β-actin (*upper image*).

The detection of HHV-6 in the eye might not be clinically relevant. HHV-6 can latently reside in cells of the lymphoid and myeloid lineage and it may have entered the inflamed eye via immune cells, similar to EBV and human immunodeficiency virus.[3,22,23] Thus, HHV-6 DNA has been detected in circulating T cells, monocytes, and leukocytes and may simply have been carried into the eyes in the inflammatory cells as a result of destruction of the blood-retina barrier. Our data indicate that most HHV-6 DNA in intraocular fluids of inflamed eyes might be a consequence of the release of HHV-6 DNA from resident ocular cells caused by intraocular inflammation. A high copy number of HHV-6 DNA was detected in patients with severe ocular inflammation, pan- or posterior uveitis, or endophthalmitis (Tables 1 and 2). This is supported by the findings of Arao et al.,[24] who showed that HHV-6 can infect human retinal pigment epithelial cells.

We detected HHV-6 in only one patient with an ocular surface inflammatory disorder. The patient was a young healthy donor suffering from atopic dermatitis. Okuno et al.[9] recently reported that 14 of 22 patients with corneal inflammation were positive for HHV-6, suggesting that the association of HHV-6 with disease was more frequent than with other herpes viruses, such as HSV-1. Thus, HHV-6 may be another sole causative agent of corneal inflammation.

HHV-6 reactivation frequently accompanies CMV reactivation,[25] and the presence of HHV-6A DNA in the eye may simply reflect the immunocompromised state of the patient. Case 6 in this study was a patient with CMV retinitis who was also found to be HHV-6A DNA-positive; however, with the exception of this patient, our HHV-6 PCR-positive patients were neither young nor immunosuppressed. We previously used multiplex PCR to search for HHV-6 in ocular fluids from 100 patients with uveitis and detected HHV-6A DNA in one patient with severe unilateral uveitis (case 1).[7] This patient's ocular fluid also contained antibodies to *Toxocara canis* larvae and we finally diagnosed ocular toxocariasis and HHV6-related panuveitis.[7] In this study, 7 patients were found to have other infectious agents, including bacteria, other herpes viruses (HSV-1), and parasites (*Toxocara*); however, it is unclear whether HHV-6 was the predominant pathogen. It is assumed that HHV-6 infections play a secondary role in the pathogenesis of ocular inflammation. Therefore, we tested intraocular samples for the presence of HHV-6 mRNA. Additional tests for HHV-6 RNA or protein in ocular tissues would have been more definitive and provided evidence of HHV-6 replication. We found HHV-6A mRNA and a high copy number of HHV-6 DNA in the same sample from a patient with ocular toxocariasis (case 1). As far as we know, this is the first report of detection of both HHV-6 DNA and mRNA in an ocular sample. The RT-PCR assay can reliably differentiate between latent and actively replicating HHV-6 and its use should allow an insight into the pathogenesis of this ubiquitous virus as previously reported.[21]

In conclusion, ocular samples collected from patients with infectious ocular disorders can contain a high copy number of HHV-6 DNA. The HHV-6–positive case was found to have HHV-6 DNA and mRNA in the inflamed eye. We are currently conducting experiments to determine whether HHV-6 type A and type B can infect ocular cells, such as retinal pigment epithelium, in vitro. Infected ocular cells can produce inflammatory cytokines and chemokines that differ from those in normal uninfected cells.

Acknowledgments

Kenji Nagata (Department of Ophthalmology, Kyoto Prefectural University of Medicine) and Yu Kaneko (Department of Ophthalmology, Yamagata University) collected and sent the samples used in this study. We are grateful for the expert technical assistance of Shizu Inoue.

References

1. Qavi HB, Green MT, Pearson G, Ablashi D. Possible role of HHV-6 in the development of AIDS retinitis. *In Vivo*. 1994;8:527–532.
2. Fillet AM, Reux I, Joberty C, et al. Detection of human herpes virus 6 in AIDS-associated retinitis by means of in situ hybridization, polymerase chain reaction and immunohistochemistry. *J Med Virol*. 1996;49:289–295.
3. Mitchell SM, Fox JD, Tedder RS, Gazzard BG, Lightman S. Vitreous fluid sampling and viral genome detection for the diagnosis of viral retinitis in patients with AIDS. *J Med Virol*. 1994;4:336–340.
4. de Groot-Mijnes JD, de Visser L, Zuurveen S, et al. Identification of new pathogens in the intraocular fluid of patients with uveitis. *Am J Ophthalmol*. 2010;150:628–636.

5. Cohen JI, Fahle G, Kemp MA, Apakupakul K, Margolis TP. Human herpesvirus 6-A, 6-B, and 7 in vitreous fluid samples. *J Med Virol.* 2010;82:996-999.
6. Maslin J, Bigaillon C, Froussard F, Enouf V, Nicand E. Acute bilateral uveitis associated with an active human herpesvirus-6 infection. *J Infect.* 2007;54:237-240.
7. Sugita S, Shimizu N, Kawaguchi T, Akao N, Morio T, Mochizuki M. Identification of human herpesvirus 6 in a patient with severe unilateral panuveitis. *Arch Ophthalmol.* 2007;125: 1426-1427.
8. de Boer JH, Verhagen C, Bruinenberg M, et al. Serologic and polymerase chain reaction analysis of intraocular fluids in the diagnosis of infectious uveitis. *Am J Ophthalmol.* 1996;121: 650-658.
9. Okuno T, Hooper LC, Ursea R, et al. Role of human herpes virus 6 in corneal inflammation alone or with human herpesviruses. *Cornea.* 2011;30:204-207.
10. Mechai F, Boutolleau D, Manceron V, et al. Human herpesvirus 6-associated retrobulbar optic neuritis in an HIV-infected patient: response to anti-herpesvirus therapy and long-term outcome. *J Med Virol.* 2007;79:931-934.
11. Moschettini D, Franceschini R, Vaccaro NM, et al. Human herpesvirus-6B active infection associated with relapsing bilateral anterior optic neuritis. *J Clin Virol.* 2006;37:244-247.
12. Oberacher-Velten IM, Jonas JB, Jünemann A, Schmidt B. Bilateral optic neuropathy and unilateral tonic pupil associated with acute human herpesvirus 6 infection: a case report. *Graefes Arch Clin Exp Ophthalmol.* 2005;243:175-177.
13. Schirmer EC, Wyatt LS, Yamanishi K, Rodriguez WJ, Frenkel N. Differentiation between two distinct classes of viruses now classified as human herpesvirus 6. *Proc Natl Acad Sci U S A.* 1991;88:5922-5926.
14. Huang LM, Kuo PF, Lee CY, Chen JY, Liu MY, Yang CS. Detection of human herpesvirus-6 DNA by polymerase chain reaction in serum or plasma. *J Med Virol.* 1992;38:7-10.
15. Suga S, Yazaki T, Kajita Y, Ozaki T, Asano Y. Detection of human herpesvirus 6 DNAs in samples from several body sites of patients with exanthem subitum and their mothers by polymerase chain reaction assay. *J Med Virol.* 1995;46:52-55.
16. Sugita S, Shimizu N, Watanabe K, et al. Use of multiplex PCR and real-time PCR to detect human herpes virus genome in ocular fluids of patients with uveitis. *Br J Ophthalmol.* 2008; 92:928-932.
17. Sugita S, Iwanaga Y, Kawaguchi T, et al. Detection of herpesvirus genome by multiplex polymerase chain reaction (PCR) and real-time PCR in ocular fluids of patients with acute retinal necrosis. *Nippon Ganka Gakkai Zasshi.* 2008;112:30-38.
18. Sugita S, Shimizu N, Watanabe K, et al. Diagnosis of bacterial endophthalmitis by broad-range quantitative polymerase chain reaction. *Br J Ophthalmol.* 2011;95:345-349.
19. Razonable RR, Fanning C, Brown RA, et al. Selective reactivation of human herpesvirus 6 variant a occurs in critically ill immunocompetent hosts. *J Infect Dis.* 2002;185: 110-113.
20. Boutolleau D, Duros C, Bonnafous P, et al. Identification of human herpesvirus 6 variants A and B by primer-specific real-time PCR may help to revisit their respective role in pathology. *J Clin Virol.* 2006;35:257-263.
21. Norton RA, Caserta MT, Hall CB, Schnabel K, Hocknell P, Dewhurst S. Detection of human herpesvirus 6 by reverse transcription-PCR. *J Clin Microbiol.* 1999;37:3672-3675.
22. Rothova A, de Boer JH, Ten Dam-van NH , et al. Usefulness of aqueous humor analysis for the diagnosis of posterior uveitis. *Ophthalmology.* 2008;115:306-311.
23. Ongkosuwito JV, Van der Lelij A, Bruinenberg M, et al. Increased presence of Epstein-Barr virus DNA in ocular fluid samples from HIV negative immunocompromised patients with uveitis. *Br J Ophthalmol.* 1998;82:245-251.
24. Arao Y, Soushi S, Sato Y, et al. Infection of a human retinal pigment epithelial cell line with human herpesvirus 6 variant A. *J Med Virol.* 1997;53:105-110.
25. Humar A, Malkan G, Moussa G, Greig P, Levy G, Mazzulli T. Human herpesvirus-6 is associated with cytomegalovirus reactivation in liver transplant recipients. *J Infect Dis.* 2000; 181:1450-1453.